

NACA RM E50E03a

NACA

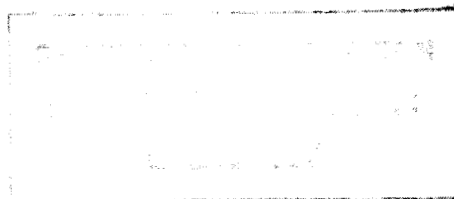
# RESEARCH MEMORANDUM

**LTVM TECH. INFORMATION CENTER**

EXPERIMENTAL INVESTIGATION OF SPREADING CHARACTERISTICS  
OF CHOKED JETS EXPANDING INTO QUIESCENT AIR

By Morris D. Rouso and Fred D. Kochendorfer

Lewis Flight Propulsion Laboratory  
Cleveland, Ohio



CLASSIFIED BY 1000000

CLASSIFICATION CHANGED TO

Restriction/Classification Cancelled

UNCLASSIFIED

DATE 8-23-54

AUTHORITY MR. J.W. CROWLEY  
CHANGE NO. 2533

Information of the United States Government, whether or not it is marked as such, is to be kept secret and is not to be disclosed to the public in any manner or by any means without the express written permission of the Federal Government. This memorandum is exempt from public release under Executive Order 11652, and its contents are to be controlled by the Federal Government. It is the policy of the Federal Government to protect its information from unauthorized disclosure to the public, and it is the duty of all persons to whom this information is disclosed to keep it secret and to prevent its unauthorized disclosure to the public. It is the policy of the Federal Government to protect its information from unauthorized disclosure to the public, and it is the duty of all persons to whom this information is disclosed to keep it secret and to prevent its unauthorized disclosure to the public.

NATIONAL ADVISORY COMMITTEE  
FOR AERONAUTICS

WASHINGTON

August 9, 1950

RM E50E03a

NATIONAL ADVISORY COMMITTEE FOR AERONAUTICS

RESEARCH MEMORANDUM

EXPERIMENTAL INVESTIGATION OF SPREADING CHARACTERISTICS

OF CHOKED JETS EXPANDING INTO QUIESCENT AIR

By Morris D. Rousso and Fred D. Kochendorfer

SUMMARY

Investigations have been conducted to determine by means of total-pressure surveys the boundaries of single and twin jets discharging through convergent nozzles into quiescent air. The jet boundaries for the region from the nozzle outlets to a station 6 nozzle diameters downstream are presented for nozzle pressure ratios ranging from 2.5 to 16.0 and for twin-jet nozzle center-line spacings ranging from 1.42 to 2.50 nozzle diameters. The effects of these parameters on the interaction of twin jets are discussed.

In order to ascertain the utility of the results for other than the test conditions, the effects of jet temperature, Reynolds number, and humidity on the pressure boundaries have been briefly investigated. The results indicate that for a jet temperature ratio of 2.6 the pressure boundaries are slightly smaller than those of corresponding unheated jets and that the effects of Reynolds number and humidity are negligible.

INTRODUCTION

Aircraft designed for transonic and supersonic speeds require extremely high-powered jet-propulsion engines and, depending on the particular requirements of a given design, single or multiple jets may be used. From a drag standpoint, it is desirable that the engine-body combination be as compact as possible. This consideration frequently leads to installations wherein the jets discharge in close proximity to the aircraft.

A considerable amount of spreading may occur in the immediate vicinity of the discharging jets, particularly at high engine-compression ratios. If any aircraft surfaces are located in this

zone, serious structural problems may arise as a result of heating of these surfaces by the hot jets. In addition, the control surfaces may be affected by the aerodynamic disturbances in the jet wake. When more than one engine is used, another complication arises from the interaction between the jets. In order to properly locate such jets, it is necessary to know the wake characteristics over a wide range of operating conditions.

Although the characteristics of subsonic jets have been thoroughly studied (references 1 and 2 give recent developments and bibliography), little information is available on the boundaries of sonic and supersonic jets, particularly in those cases for which the pressure is less in the discharge region than at the nozzle outlet. Investigations are consequently being conducted at the NACA Lewis laboratory to study the spreading characteristics of jets. One phase of this program was concerned with total-temperature profiles for twin jets (reference 3). Jet characteristics studied by means of total-pressure surveys are presented herein. The effects of nozzle pressure ratio, nozzle temperature ratio, and jet spacing for single and twin jets discharging through convergent nozzles into quiescent air are evaluated. A limited study is made of the effects of Reynolds number and humidity on the jet boundaries.

#### SYMBOLS

The following symbols are used in this report:

$D_n$  nozzle-throat diameter

$M_j$  theoretical jet Mach number,  $M_j = \left\{ \frac{2}{\gamma-1} \left[ \left( \frac{P_p}{P_0} \right)^{\frac{\gamma-1}{\gamma}} - 1 \right] \right\}^{1/2}$

$M$  Mach number at any point in jet

$P$  total pressure

$p$  static pressure

$R$  ratio of radial distance from jet center line to nozzle diameter

$Re$  Reynolds number

$S$  distance between center lines of twin jets

$T$  total temperature

- 1322
- X ratio of distance from plane containing center lines of twin jets to nozzle diameter
- Y ratio of distance from plane of symmetry between jets to nozzle diameter
- Z ratio of axial distance downstream of nozzle outlets to nozzle diameter
- $\gamma$  ratio of specific heats

Subscripts:

- O ambient
- p nozzle inlet
- r rake

APPARATUS AND PROCEDURE

The apparatus used in the investigations (fig. 1) consisted essentially of a primary chamber, several sets of axially symmetric convergent nozzles, and a low-pressure receiver.

The primary chamber could be opened to the atmosphere or connected to either the compressed-air system or the dry-air system. The pressure at the nozzle inlet  $P_p$  was measured by four total-pressure tubes in the primary chamber. The spacing between the nozzles  $S$  was 1.42 inches for all twin-jet studies. Nozzle diameters were chosen to give values of the spacing parameter  $S/D_n$  of 1.42, 1.738, and 2.50. Single-jet studies were made by plugging one of the nozzles. The low-pressure receiver had an 8- by 9-inch cross section. The receiver was connected to the laboratory exhaust system, and any pressure between atmospheric and 2.5 inches of mercury absolute could be obtained by throttling. The receiver pressure  $p_0$  was measured by static orifices in the tank wall. Pressures in the jet were measured by a 23-tube total-pressure rake. Each total-pressure tube was parallel to the nozzle axis.

For the humidity and Reynolds number investigations the primary chamber was connected to the dry-air and high-pressure systems, respectively. For all other investigations the primary chamber was open to the atmosphere and the nozzle pressure ratio  $P_p/p_0$  was set at values



of 2.5, 4.6, 10, and 16 by adjusting the receiver pressure. The effect of temperature on jet spreading was investigated by burning propane in the primary chamber.

A complete total-pressure survey was made in one quadrant of the wake and sufficient points in adjacent quadrants were investigated to ascertain symmetry. Surveys were made at stations 1, 2, 4, and 6 nozzle diameters downstream of the nozzle outlets.

#### DEFINITION OF JET BOUNDARY

Because the velocity in the outer fringe of the jet approaches zero asymptotically, the jet boundary is arbitrarily defined as the locus of points for which the Mach number ratio  $M/M_j$  attains a value of 0.11, where  $M$  is the Mach number at any point in the jet fringe and  $M_j$  is the theoretical jet Mach number corresponding to isentropic expansion from  $P_p$  to  $p_0$ . Although arbitrary, the Mach number ratio of 0.11 was selected because of convenience in measuring technique.

For the boundary regions of the jet the value of  $M$  is subsonic and it can be assumed that the pressure measured by the rake is the true total pressure. It can also be assumed that the static pressure in the boundary region is equal to the receiver pressure  $p_0$ . The value of the rake-pressure ratio for points near the boundary is then given by

$$\frac{p_0}{P_r} = \left\{ \frac{1}{1 + \left(\frac{M}{M_j}\right)^2 \left[ \left(\frac{P_p}{p_0}\right)^{\frac{\gamma-1}{\gamma}} - 1 \right]} \right\}^{\frac{\gamma}{\gamma-1}} \quad (1)$$

The ratio  $p_0/P_r$  is plotted in figure 2 as a function of  $P_p/p_0$  for several values of  $M/M_j$ . The values of  $M/M_j$  given by equation (1) lose significance in regions of the jet where  $p_0/P_r$  is less than 0.53, because for these regions the value of  $M$  is supersonic and the pitot-pressure readings are subject to shock losses. For this reason only the subsonic portion of the jets is considered.

1322

For each position of the rake, the location of the point for which  $M/M_j = 0.11$  was obtained by plotting the value of  $p_0/p_r$  for each tube as a function of tube position. As an example, in figure 3 the value of  $p_0/p_r$  is plotted as a function of tube position  $X$  for a nozzle pressure ratio of 16; consequently, the value of  $p_0/p_r$  for  $M/M_j = 0.11$  is 0.950 (fig. 2). The value of  $X$  corresponding to  $M/M_j = 0.11$  is therefore  $1.50 D_n$ .

## RESULTS AND DISCUSSION

### Unheated Single Jet

The boundaries of an unheated single jet are given in figure 4 for an axial station 1 nozzle diameter downstream of the nozzle outlet ( $Z = 1$ ) for a range of nozzle pressure ratios. These boundaries were obtained by cross-plotting the points on the rake-survey pressure distributions for which  $M/M_j = 0.11$ . The boundaries so defined are adequately represented by circles which are concentric with the nozzle and, consequently, a single radius can be used to define each boundary.

Values for the radii of the jet boundaries were determined in a similar manner for downstream stations of 2, 4, and 6 diameters and the results are shown in figures 5 and 6. The boundaries of figure 5 are given as functions of axial distance from the nozzle outlet for several values of nozzle pressure ratio  $P_p/p_0$ . Increasing the pressure ratio resulted in an increased rate of expansion immediately downstream of the nozzle, as expected. Following the initial rapid expansion, the rate of growth of the jet radius decreased and appeared to vary only slightly with distance downstream.

The boundaries in figure 6 are given as functions of nozzle pressure ratio for several values of downstream station  $Z$ . The lowest value of  $P_p/p_0$  investigated in this study was 1.50. The values for  $P_p/p_0$  of 1.04 were obtained from reference 4. For the lower values of  $P_p/p_0$ , the jet radii were relatively unaffected by changes in nozzle pressure ratio and for each value of  $Z$  a value of the pressure ratio existed above which the jet radius increased. This value varied from 2.5 for  $Z = 1$  to 5.0 for  $Z = 6$ .

In order to show the correspondence between the jet boundary arbitrarily defined by the Mach number ratio 0.11 and the jet visible in a schlieren photograph, points obtained from the pressure surveys at nozzle pressure ratios of 2.5 and 16.0 have been superimposed on the corresponding photographs in figure 7. The boundary, visible in the schlieren photographs, is in close agreement with the boundary determined by the pressure survey, although as the mixing region thickens the boundary becomes less clearly defined in the schlieren.

The effect of nozzle pressure ratio on the subsonic portion of the Mach number distributions of a single jet is shown in figure 8 for several downstream stations. The curves for  $P_p/p_0$  of 2.5, 4.6, 10.0, and 16.0 were obtained from cross plots of the pressure surveys; also included are curves for  $P_p/p_0$  of 1.04 taken from the data in reference 4. These curves show that the distributions for different pressure ratios are similar, particularly for the axial stations close to the nozzle, and that the chief effect of an increase in nozzle pressure ratio is to spread the jet without altering this outer portion of the profile.

The curves from figure 8 are cross-plotted in figure 9. The positions of the lines of constant Mach number are shown as a function of distance downstream of the nozzle for several values of the nozzle pressure ratio. As the downstream distance  $Z$  increased, the radii of the constant Mach number surfaces in general increased for  $M/M_j < 0.5$  and decreased for  $M/M_j > 0.7$  for the range of  $Z$  investigated.

In order to extend the utility of the jet-boundary charts, a limited study was made of the effects of jet Reynolds number and humidity. Because the flow in the jet mixing region is turbulent, the effect of Reynolds number on the Mach number profile and on the resulting jet boundary should be small. In order to determine the magnitude of this effect, the pressure at the inlet  $P_p$  was varied and the ratio  $P_p/p_0$  was held constant. The Reynolds number of the fluid in the mixing region can also be varied by varying the nozzle-inlet temperature, the nozzle temperature ratio, or the nozzle pressure ratio. However, because a change in any of these variables causes a change in the jet boundary which may mask any change that may result from the corresponding change in the Reynolds number, the effect of Reynolds number alone can best be studied by varying the nozzle-inlet pressure and holding the other variables fixed. In this case, the Reynolds number can be defined by the stagnation density at

the nozzle inlet, the velocity and viscosity of the nozzle throat, and the nozzle-throat diameter. Changing the Reynolds number from 290,000 to 1,340,000 had no appreciable effect on the pressure distribution (fig. 10) and hence on the jet boundary. The range investigated covers the Reynolds numbers to be expected in flight.

Conceivably, a condensation shock can alter the flow in the jet and therefore humidity is another quantity that may affect the jet boundary. The atmospheric air used in the investigation had a dew point of approximately 35° F. The data of reference 5 indicate that in a wind tunnel designed for a pressure ratio of 10 a moderately strong compression shock can be expected if the dew point of the intake air is 35° F. Because of the rapid expansion and the strong compression shocks, however, the flow in the jets of the present study was different than that in a tunnel and it is possible that no condensation shocks occurred. In order to evaluate the effects of humidity, additional studies were made using relatively dry air (dew point, -20° F). The distributions for wet and dry air were almost identical (fig. 10).

#### Heated Single Jet

In order to determine to what extent the unheated-jet boundaries approximate those of heated jets, pressure surveys were made of a single jet having a total temperature of 1360° F absolute, the temperature ratio  $T_p/T_0$  being 2.6. The boundaries of the heated jets are shown in figure 11 for a range of nozzle pressure ratios. The trends were consistent with those of the unheated jet. A comparison of the jet radii for the heated and unheated single jet over a range of nozzle pressure ratios and axial stations is presented in table I. The heated-jet radius was smaller than that for the unheated jet near the nozzle outlet but increased to a value nearly equal to that of the unheated jet at 6 diameters for all cases except at a nozzle pressure ratio of 2.5, when the heated-jet boundary was smaller for all downstream stations.

#### Twin Jets

When twin jets are employed, interaction between the jets is obviously an additional factor influencing jet spreading, as illustrated in figure 12 by a comparison of the boundaries of single and twin jets operated at a pressure ratio of 16.0 at an axial station of 6 diameters. Single-jet boundaries spaced 1.738 nozzle diameters between centers have been superposed on the twin-jet boundary. The

displacement region is a result of the interaction of the twin jets. In the zone clear of the region of interaction, the jet boundaries are relatively unaffected; that is, the single- and twin-jet radii in this region nearly coincide. A comparison of these radii is presented in table I.

The extent of the jet interaction depends on both the jet nozzle pressure ratio and the nozzle spacing. These effects were investigated quantitatively and the results are presented in figures 13 to 17.

Nozzle pressure ratio. - For a nozzle spacing of 1.738 diameters, the effect of varying the pressure ratio is shown in figure 13, where jet boundaries for several pressure ratios are presented at axial stations of 1, 2, 4, and 6 diameters. At the 1-diameter station (fig. 13(a)) the jets interacted at a pressure ratio of 10.0. The displacement region at this pressure ratio was appreciable and became even more pronounced at a pressure ratio of 16.0. For the station 6 diameters downstream of the nozzles (fig. 13(d)), the displacement region increased considerably.

Schlieren photographs showing the spreading of single and twin jets at nozzle pressure ratios of 2.5, 4.6, 10.0, and 16.0 are presented in figure 14. The twin jets pictured were spaced 1.42 nozzle diameters apart. The difference in jet thickness of the single and twin jets was particularly noticeable at a pressure ratio of 16.0 and was a direct result of the jet interaction and the resulting displacement.

Nozzle spacing. - An additional factor influencing the boundary of twin interacting jets is the distance between the nozzle axes. This effect is shown in figure 15, where boundaries are presented for twin jets having nozzle spacings  $S/D_n$  of 1.42 and 2.5, and operated at several pressure ratios at a given axial station. Increasing the spacing from 1.42 to 2.5 diameters delayed the point of jet interaction and thus decreased the displacement at the expense of widening the over-all jet boundary.

The boundaries for twin jets having nozzle spacings of 1.42, 1.738, and 2.5 and operated at a pressure ratio of 10.0 at several axial stations are shown in figure 16. The effect of spacing on jet spreading is again apparent.

The effect of nozzle spacing on jet interaction is also illustrated by the schlieren photographs in figure 17. Nozzle spacings of 1.42, 1.738, and 2.5 diameters are shown for nozzle pressure ratios

of 2.5, 4.6, 10.0, and 16.0. Similar effects on the shock interaction pattern were produced either by an increase in the pressure ratio or by a decrease in the nozzle spacing, as shown in figure 17. For example, increasing the pressure ratio from 10 to 16 for a spacing of 1.738 produced a pattern similar to that resulting from a decrease in spacing to 1.42, with the pressure ratio remaining at 10.

### SUMMARY OF RESULTS

The following results were obtained from an experimental investigation of the spreading characteristics of jets:

1. For both single and twin jets the effect of nozzle pressure ratio on the jet boundaries was significant. Increasing the nozzle pressure ratio resulted in increased expansion downstream of the nozzles. Following the initial rapid expansion, the rate of growth of the jets decreased and appeared to vary only slightly with axial distance.
2. The effect of nozzle temperature ratio on jet spreading was small throughout the range investigated. Except for a nozzle pressure ratio of 2.5, the boundaries for the heated jets were somewhat smaller at the nozzle outlet than those for the unheated jet, but at an axial station of 6 diameters the boundaries for both were identical.
3. The effect of Reynolds number in the range from 290,000 to 1,340,000 was negligible.
4. The presence of moisture in the air had no effect on the spreading of the jets for the range investigated.
5. For the twin jets, the effect of the spacing between nozzle center lines was significant. For example, changing the spacing from 1.42 to 2.50 nozzle diameters reduced the height of the boundary in the plane of symmetry between the jets from 2.10 to 1.0 diameters at an axial station of 6 diameters at the expense of widening the overall jet boundary.

Lewis Flight Propulsion Laboratory,  
National Advisory Committee for Aeronautics,  
Cleveland, Ohio.

## REFERENCES

1. Corrsin, Stanley, and Uberoi, Mahinder S.: Further Experiments on the Flow and Heat Transfer in a Heated Turbulent Air Jet. NACA TN 1865, 1949.
2. Forstall, Walton, Jr., and Shapiro, Ascher H.: Momentum and Mass Transfer in Coaxial Gas Jets. Meteor Rep. No. 39, Dept. Mech. Eng., M. I. T., July 1949. (Bur. Ord. Contract NOrd 9661.)
3. Sloop, John L., and Morrell, Gerald: Temperature Survey of the Wake of Two Closely Located Parallel Jets. NACA RM E9I21, 1950.
4. Alexander, L. G.: The Velocity Field in an Isothermal Turbulent Free Jet Adjacent to the Source. Tech. Rep. No. 3, Eng. Exp. Station, Univ. Ill., Nov. 20, 1948. (ONR Contract N6-ori-71, T.D. No. XI.)
5. Burgess, Warren C., Jr., and Seashore, Ferris L.: Criteria for Condensation-Free Flow in Supersonic Tunnels. NACA RM E9E02, 1949.

TABLE I - JET RADII FOR SINGLE AND TWIN JETS

Nozzle pressure ratio $P_p/p_0$	Axial station Z (diameters)	Jet radii for single jet, nozzle diameters		Jet radii for twin jets clear of interaction zone, nozzle diameters		
		Heated	Unheated	Nozzle spacing, $S/D_n$		
				1.42	1.738	2.5
16.0	1	1.07	1.20		1.17	
	2	1.32	1.39	1.38	1.42	1.41
	4	1.48	1.55		1.51	
	6	1.62	1.65		1.63	
10.0	1		1.05	1.00	1.02	1.00
	2	1.06	1.17	1.11	1.14	1.14
	4		1.27	1.17	1.27	1.24
	6	1.40	1.39	1.33	1.41	1.39
4.6	1		.78		.78	
	2	.77	.82	.80	.83	.81
	4		1.00		1.00	
	6	1.15	1.17		1.16	
2.5	1	.61	.64		.63	
	2	.67	.72	.71	.73	.72
	4	.82	.89		.94	
	6	1.06	1.19		1.20	
1.5	1		.64			
	2		.73			
	4		1.03			
	6		1.18			





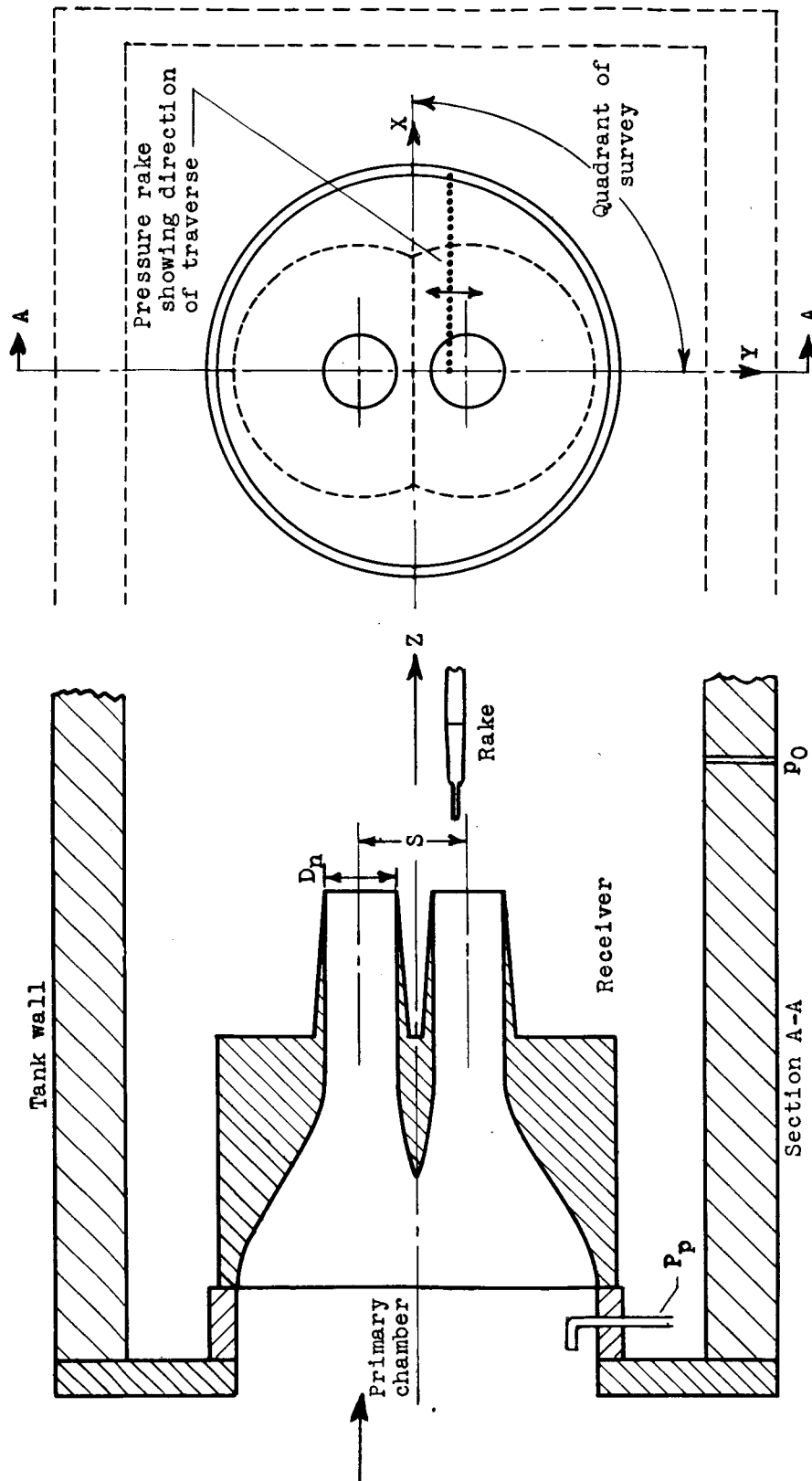


Figure 1. - Experimental assembly showing primary chamber, low-pressure receiver, convergent nozzles, and total-pressure rake.

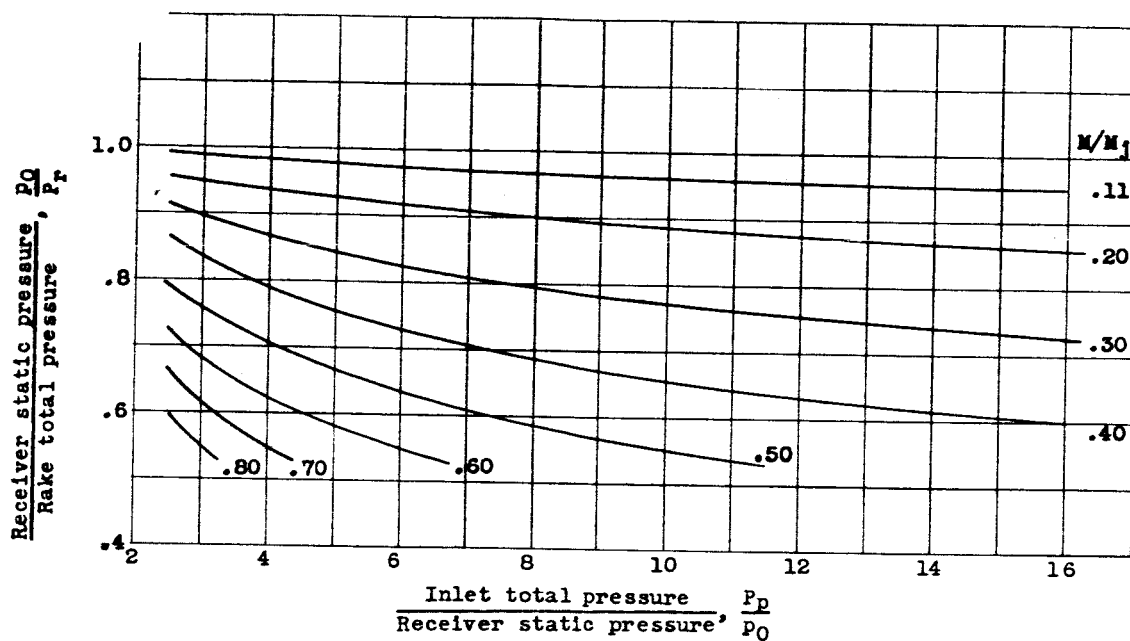


Figure 2. - Variation of rake pressure ratio with nozzle pressure ratio for several Mach number ratios. Ratio of specific heats  $\gamma$ , 1.4.

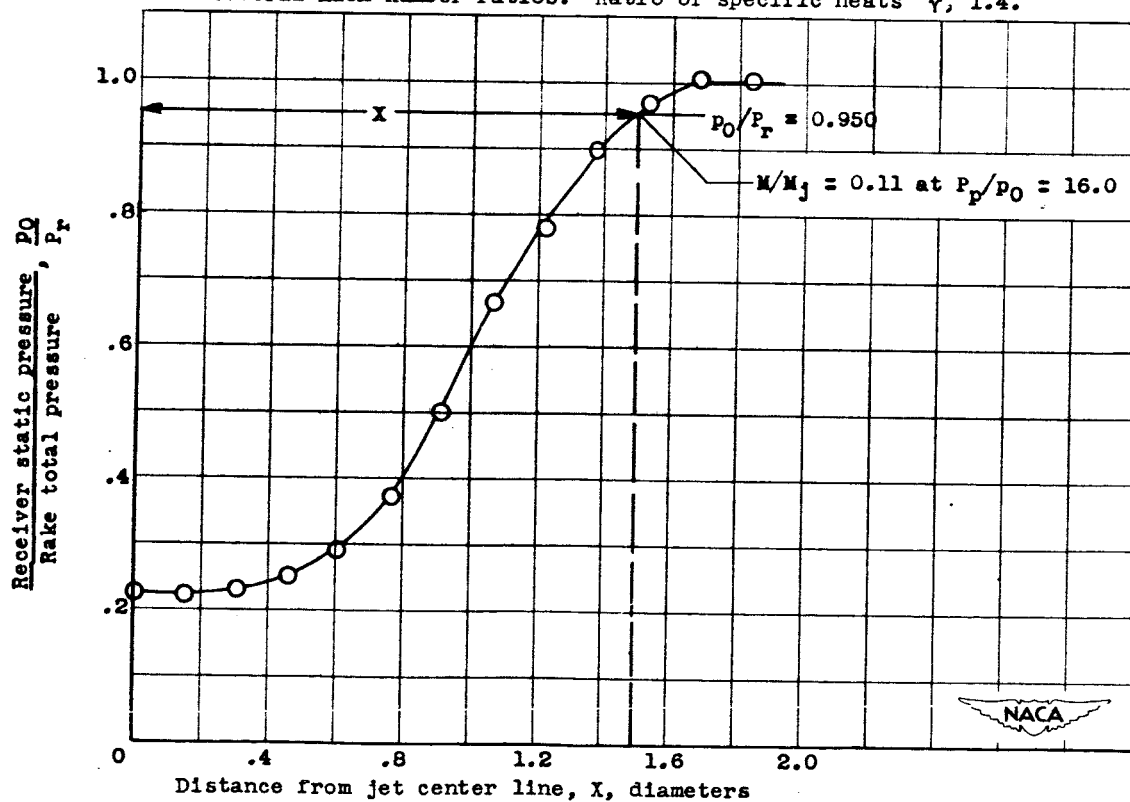


Figure 3. - Typical pressure distribution in jet wake. Nozzle pressure ratio.  $P_p/P_0$ , 16.0.

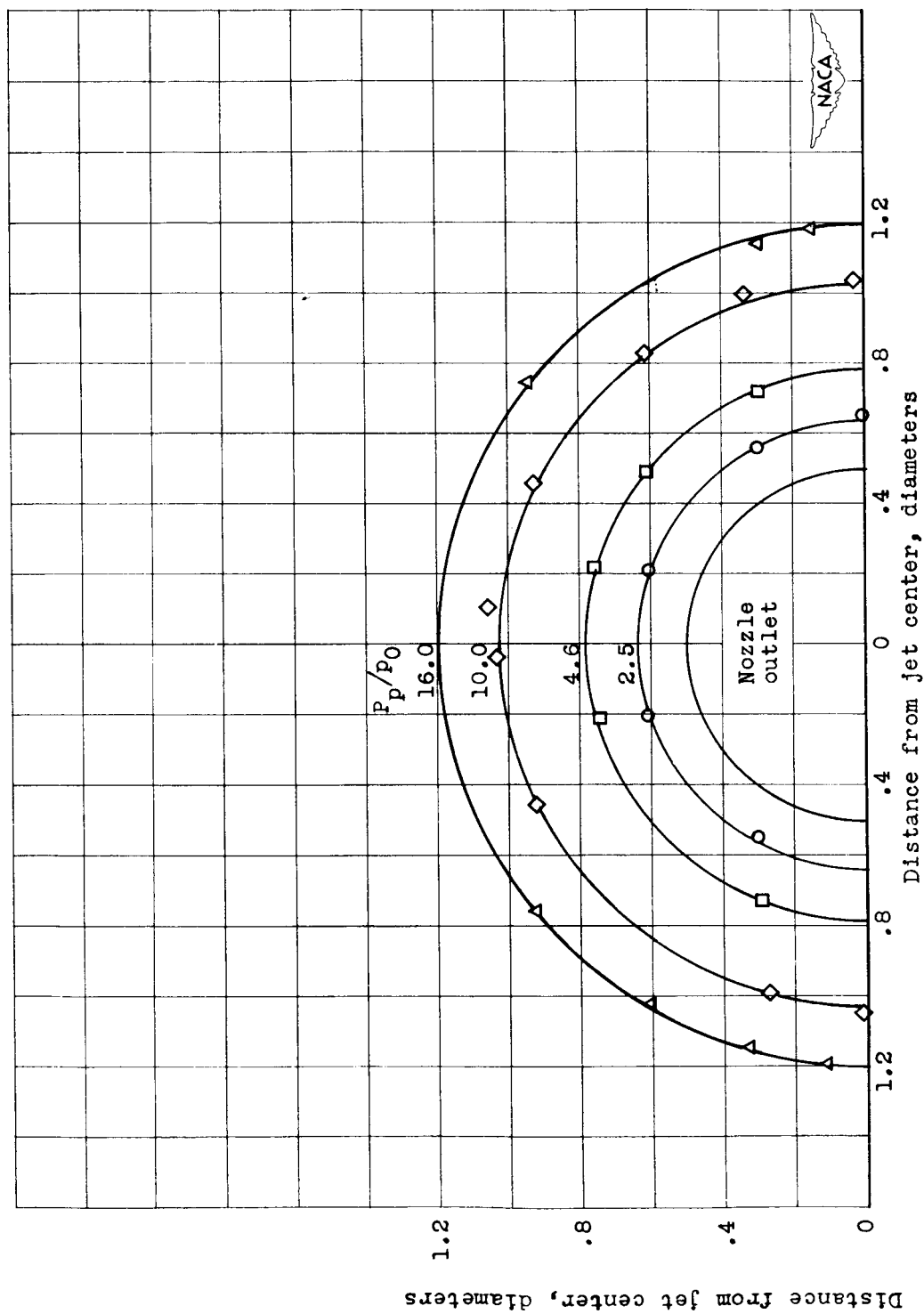


Figure 4. - Lateral boundaries for single jet. Mach number ratio  $M/M_j$ , 0.11; nozzle temperature ratio  $T_p/T_0$ , 1; axial station Z, 1 diameter.

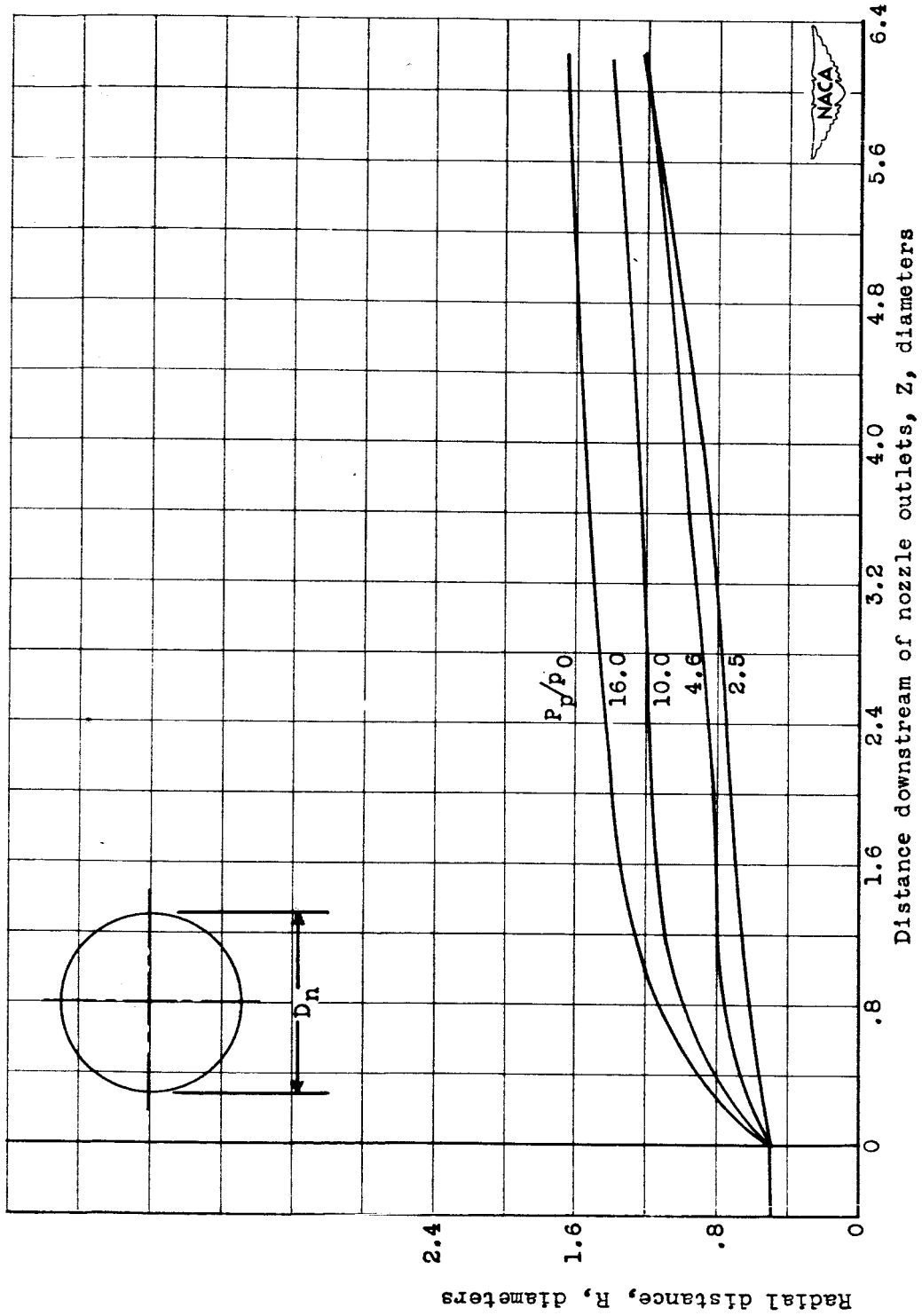


Figure 5. - Variation of jet radius with downstream distance for single jet. Mach number ratio  $M/M_j$ , 0.11; nozzle temperature ratio  $T_p/T_0$ , 1.

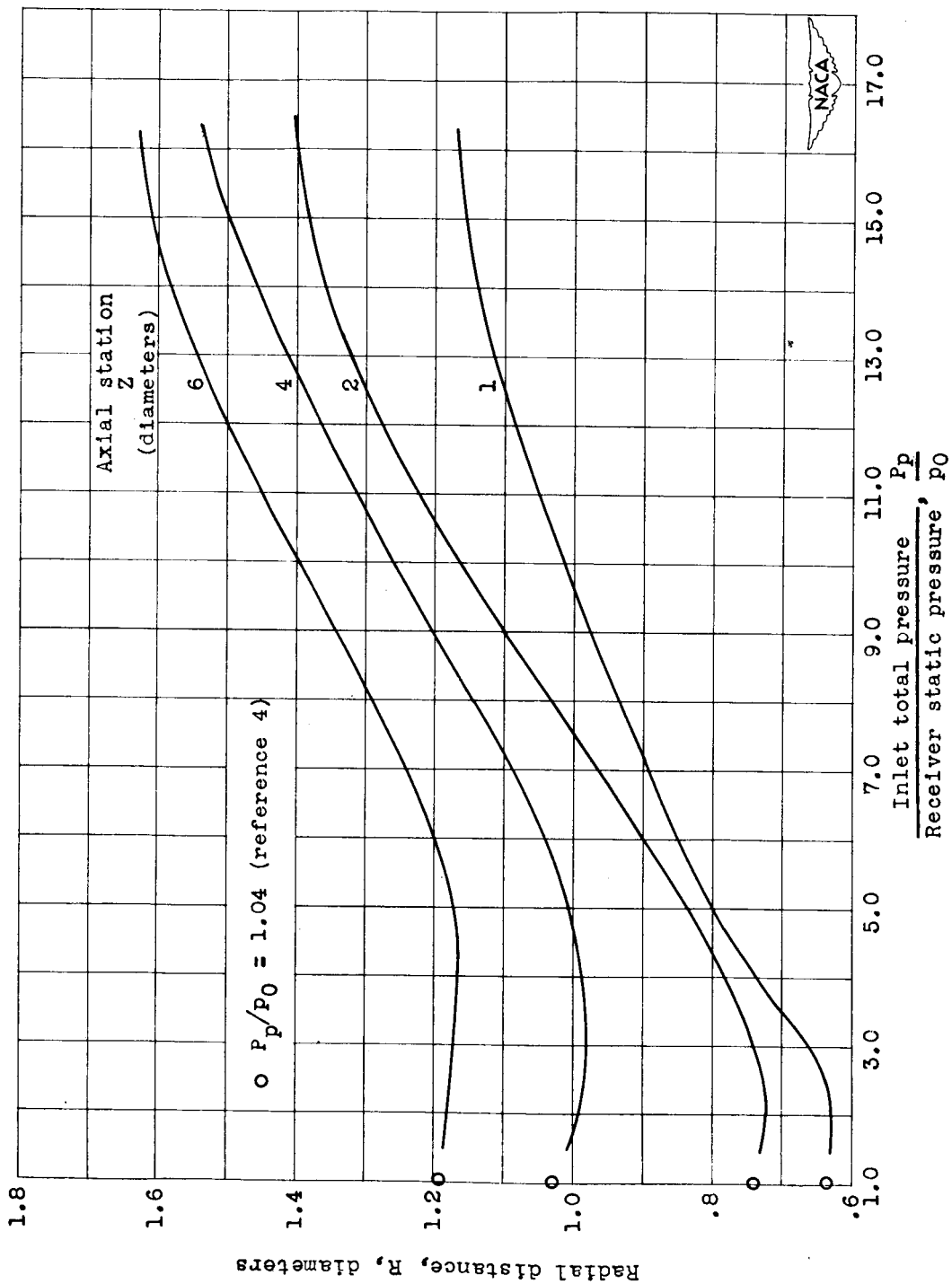
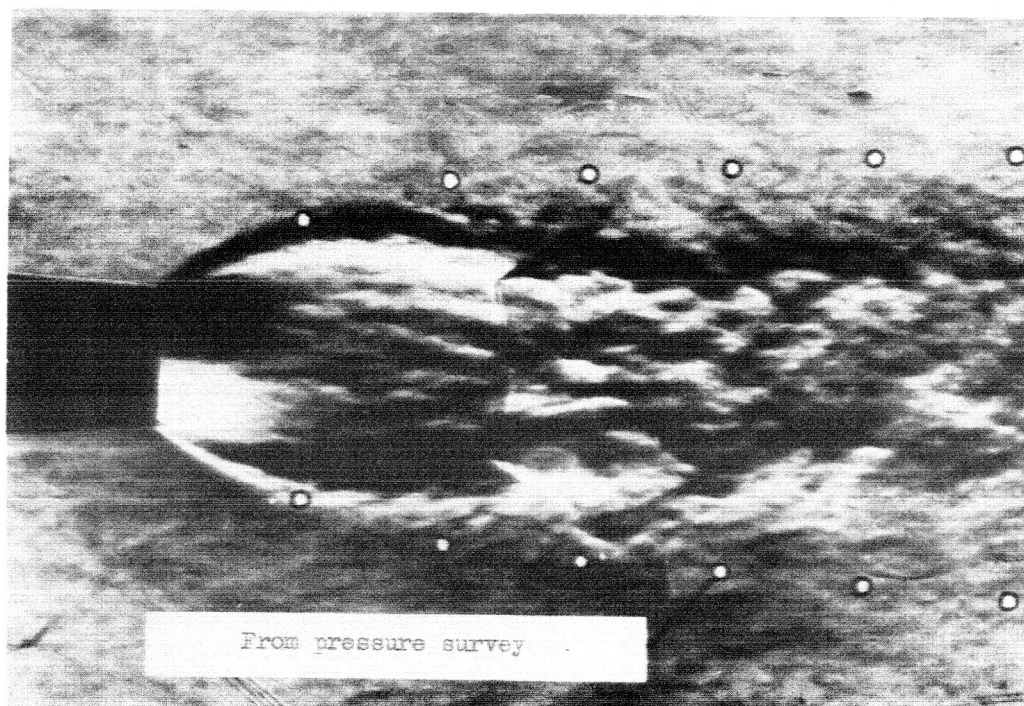
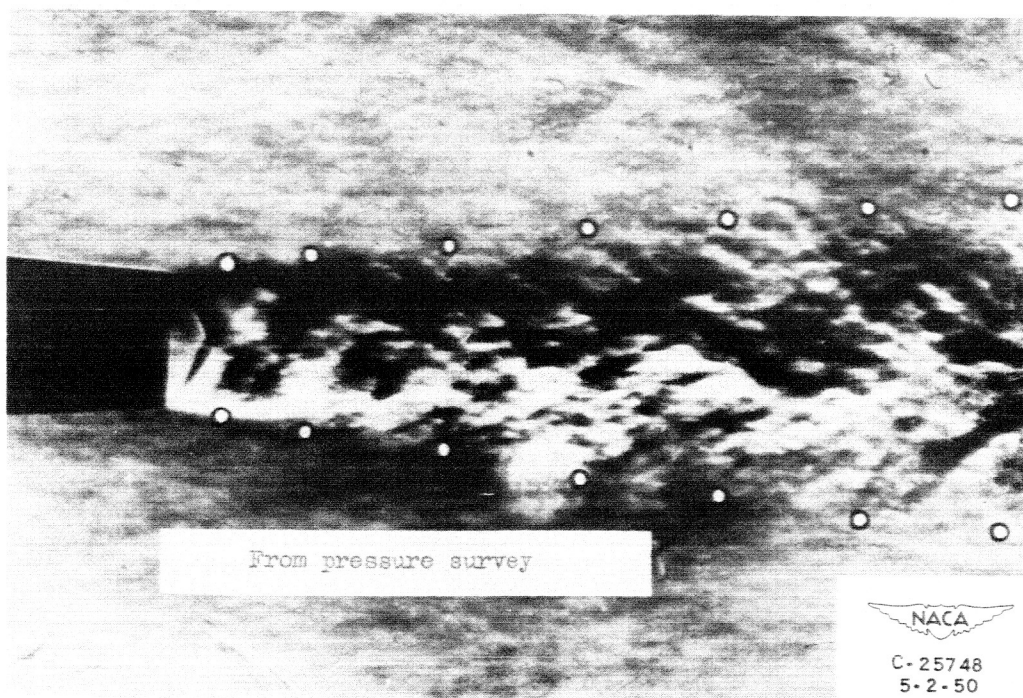


Figure 6. - Variation of jet radius with nozzle pressure ratio for single jet. Mach number ratio  $M/M_j$ , 0.11; nozzle temperature ratio  $T_p/T_0$ , 1.



(a) Nozzle pressure ratio  $P_p/P_0$ , 16.0.



(b) Nozzle pressure ratio  $P_p/P_0$ , 2.5

Figure 7. - Comparison of schlieren photographs and pressure surveys of single jet.

CONFIDENTIAL

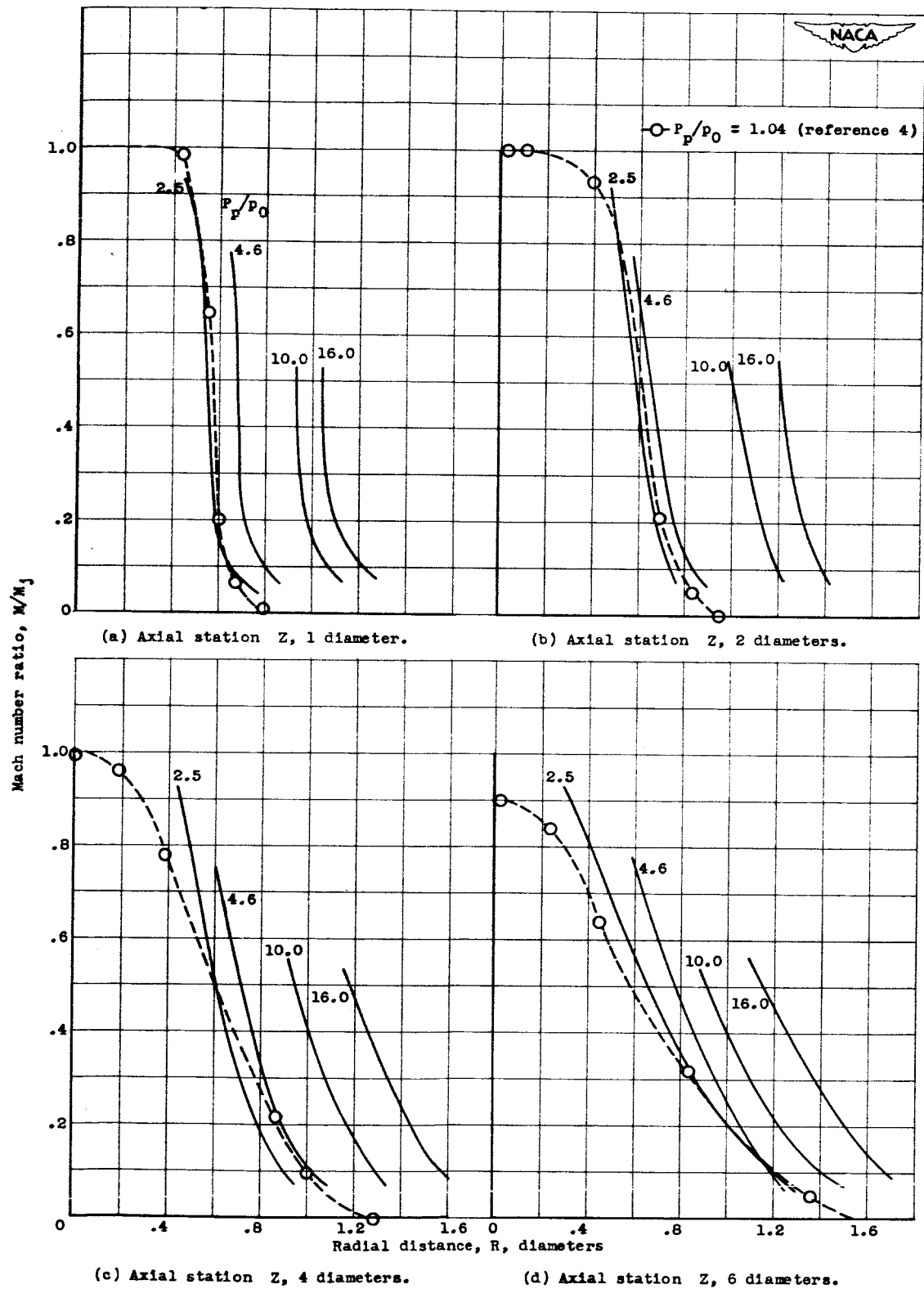


Figure 8. - Mach number distributions in single jet. Nozzle temperature ratio  $T_p/T_0$ , 1.

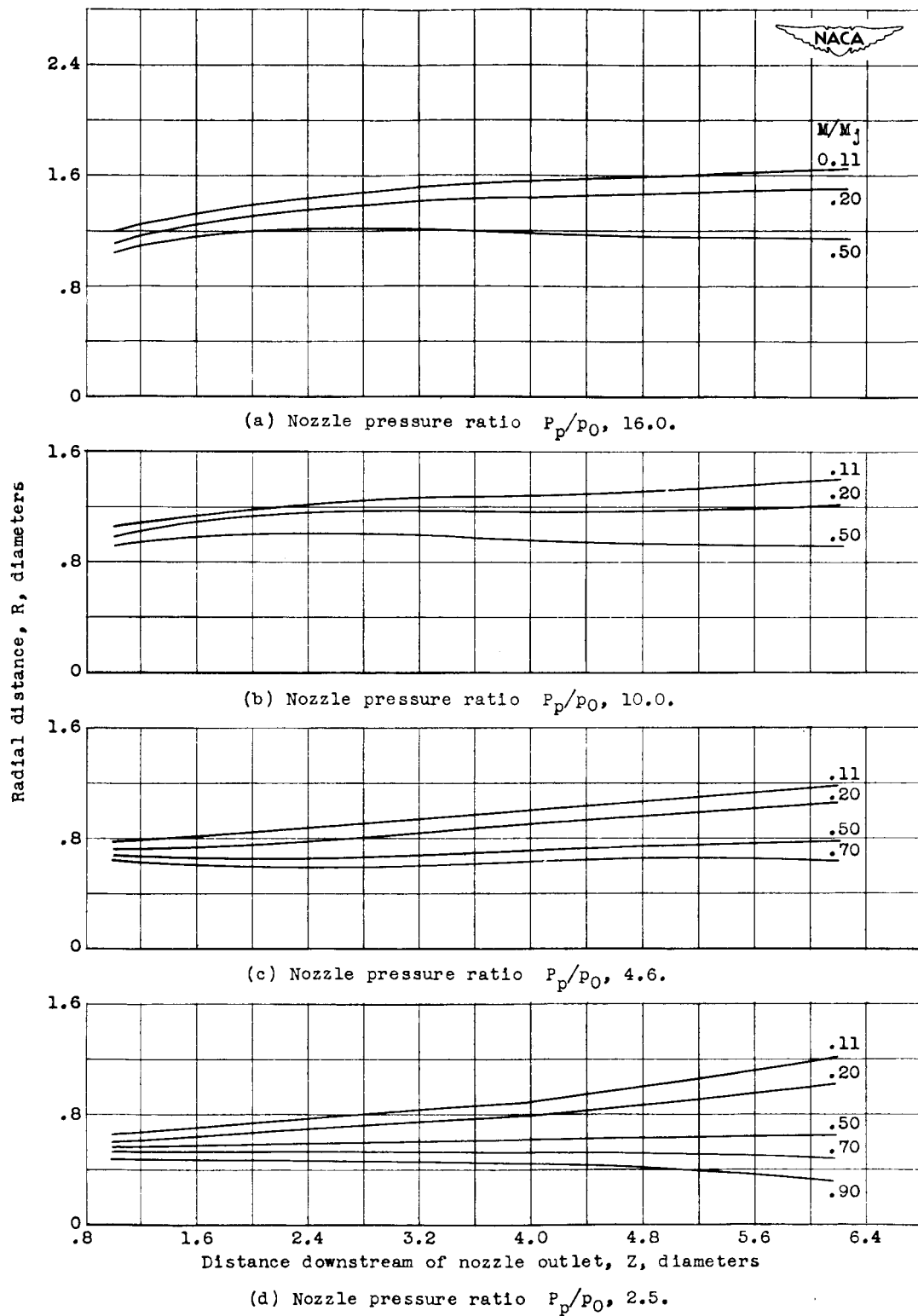


Figure 9. - Lines of constant Mach number ratio for single jet. Nozzle temperature ratio  $T_p/T_0$ , 1.



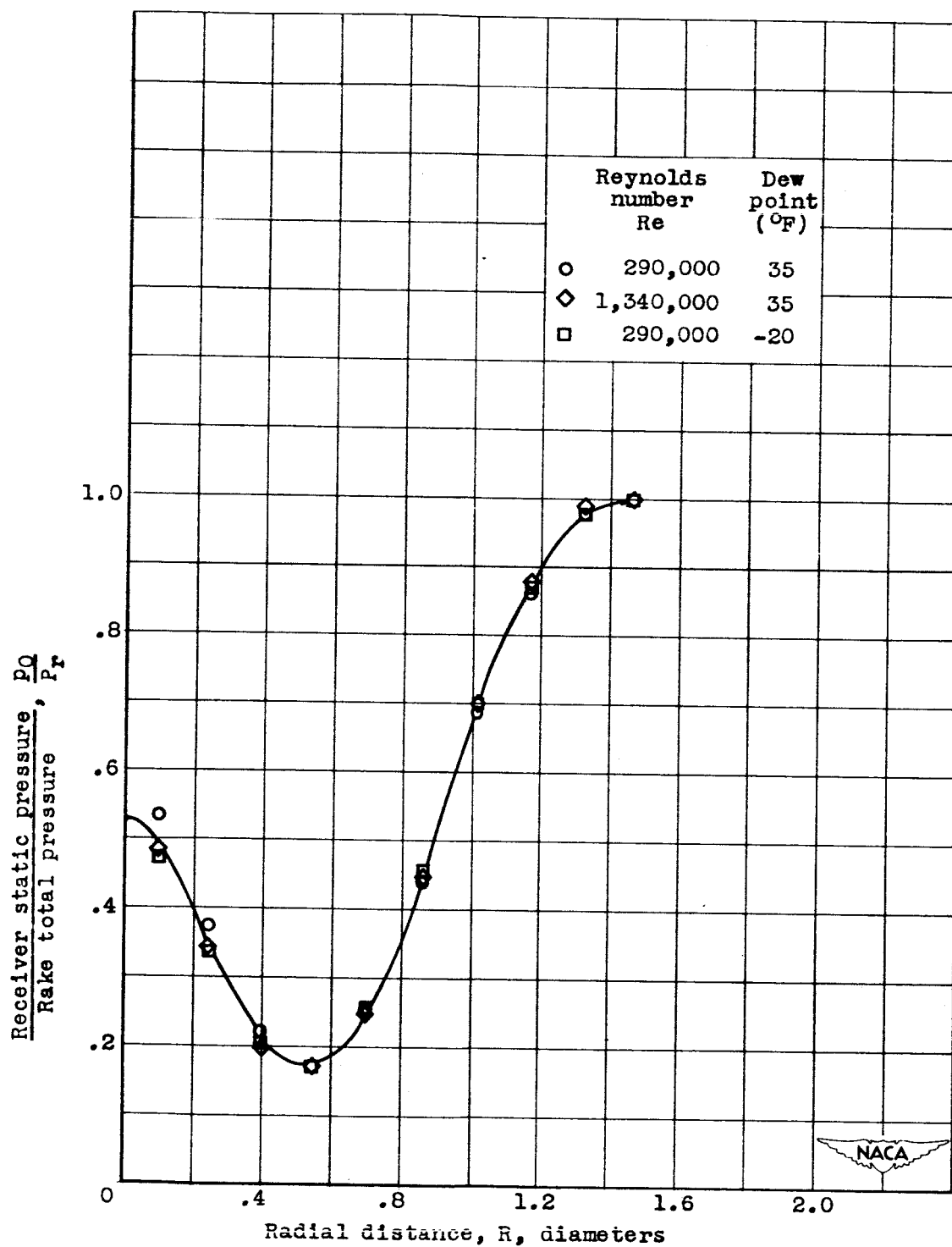


Figure 10. - Effect of Reynolds number and humidity on radial pressure distributions for single jet. Nozzle pressure ratio  $P_p/P_0$ , 10.0; nozzle temperature ratio  $T_p/T_0$ , 1; axial station  $Z$ , 4 diameters.

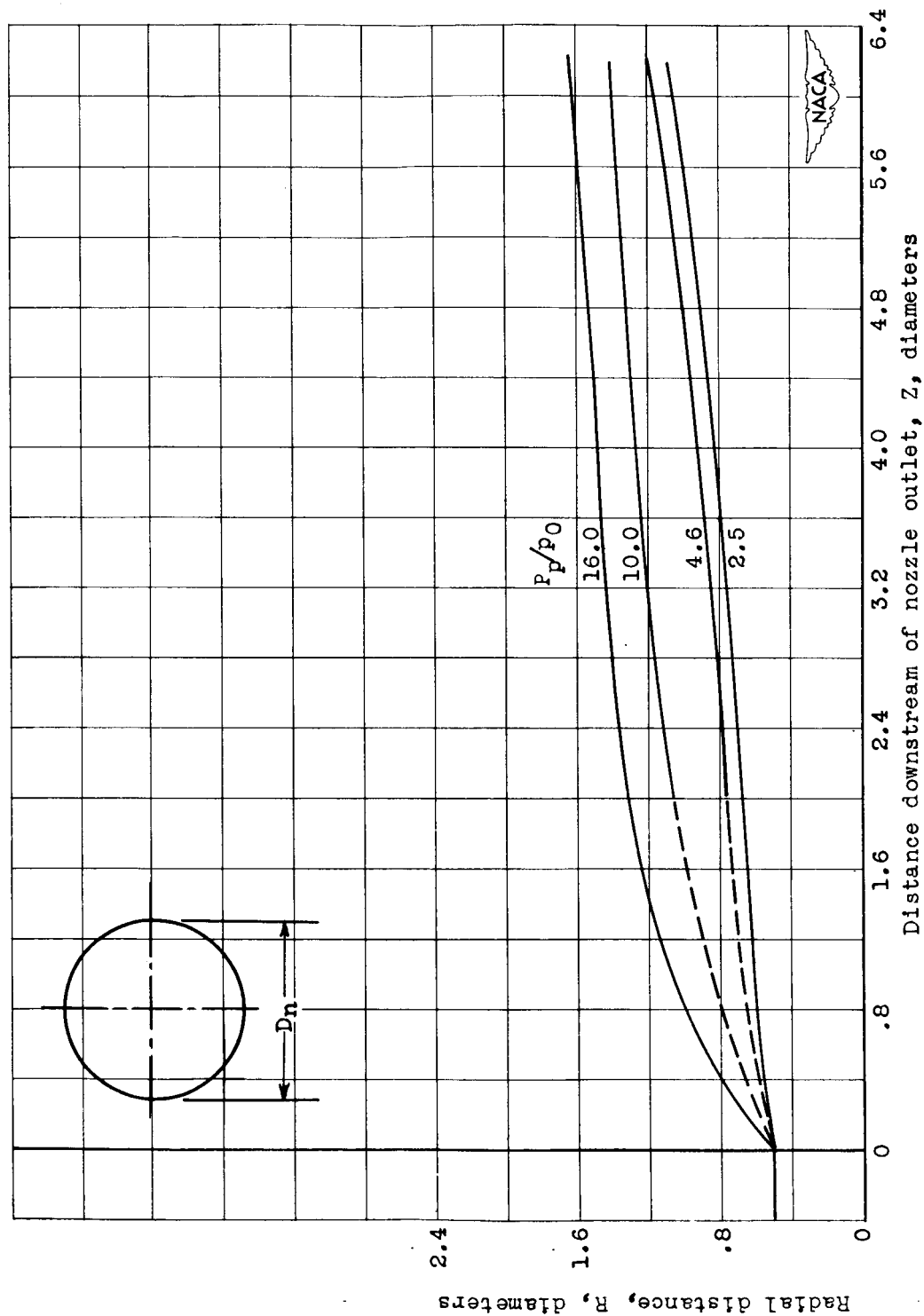


Figure 11. - Variation of jet radius with downstream distance for single heated jet. Mach number ratio  $M/M_j$ , 0.11; nozzle temperature ratio  $T_p/T_0$ , 2.6.

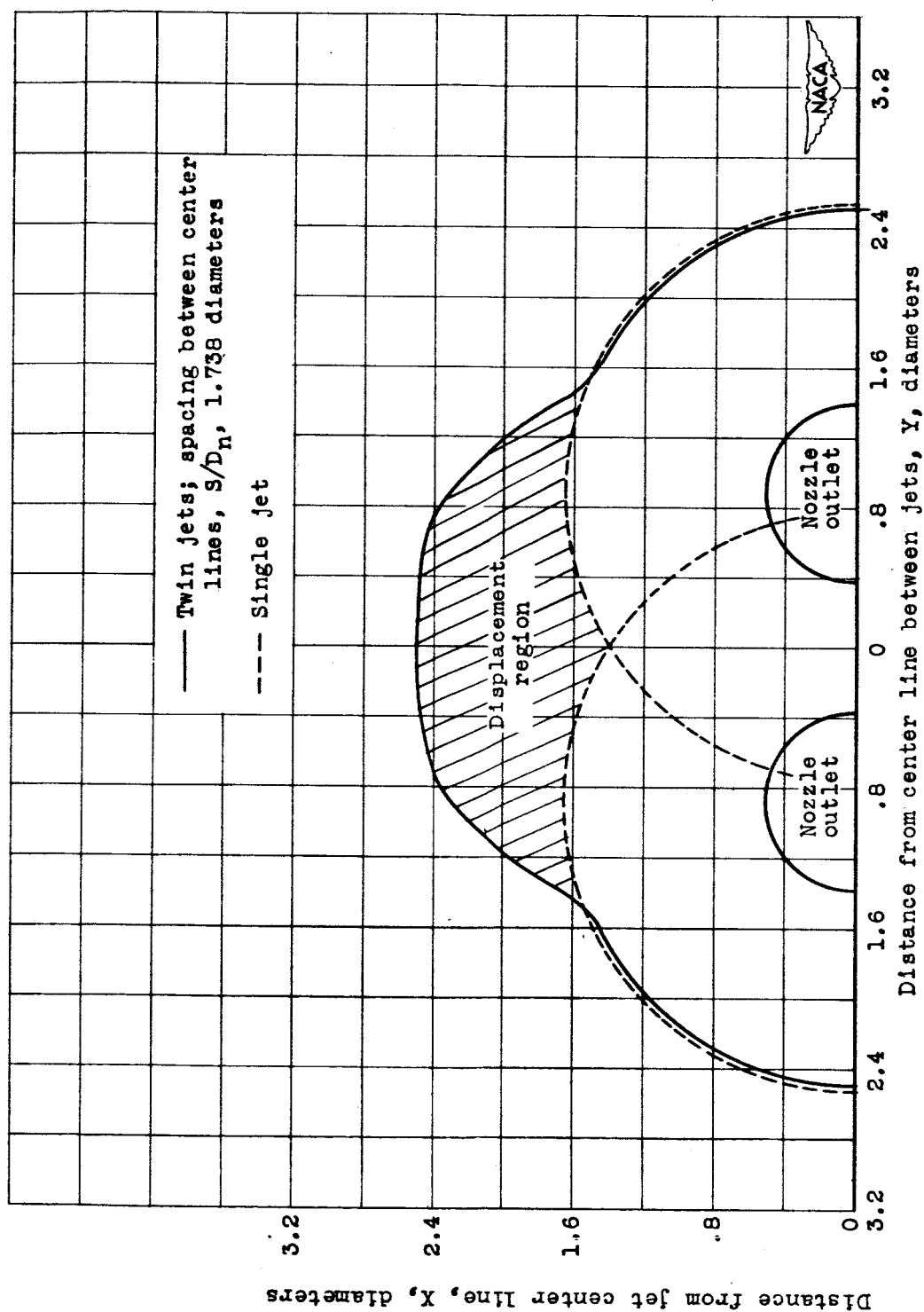
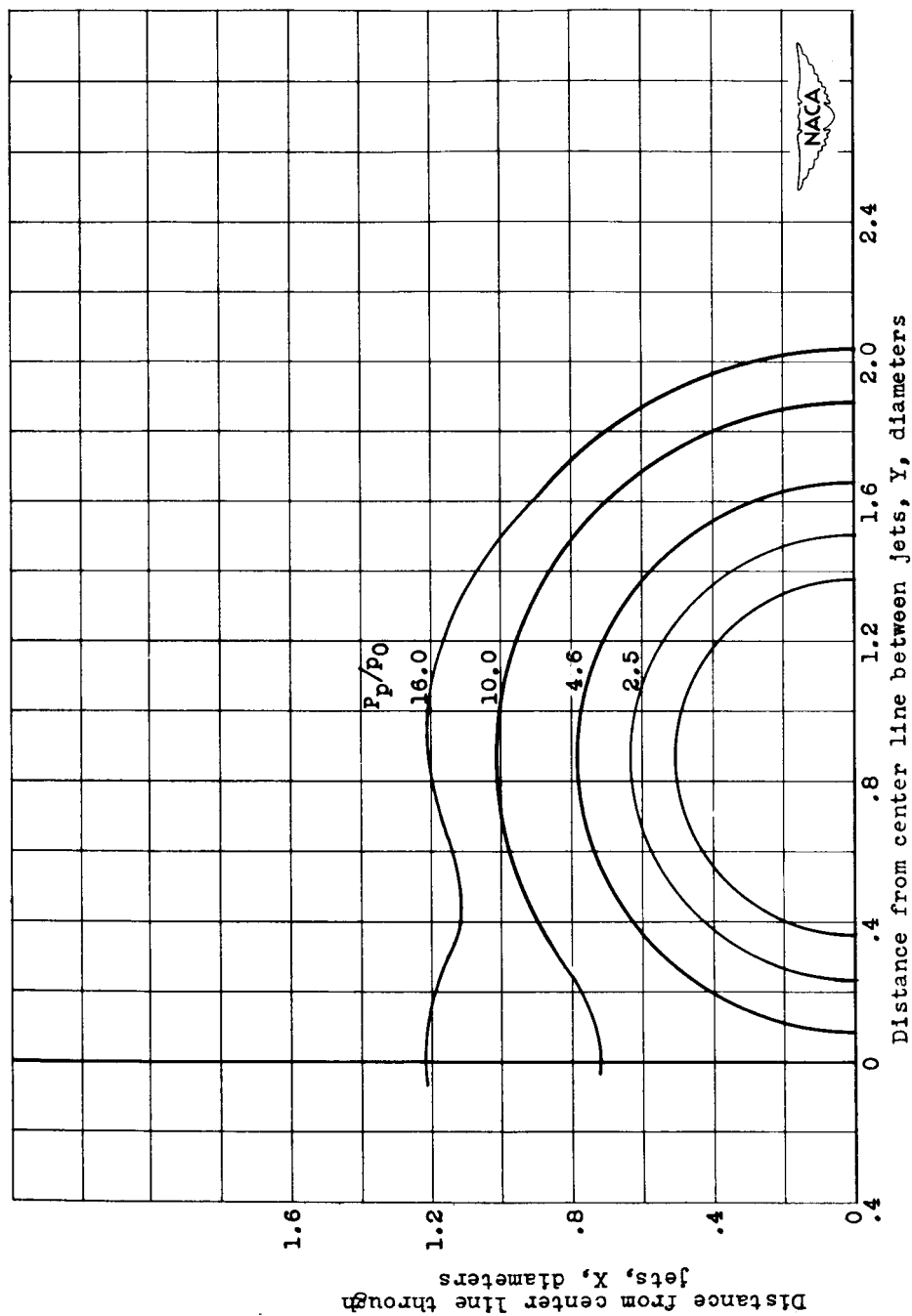
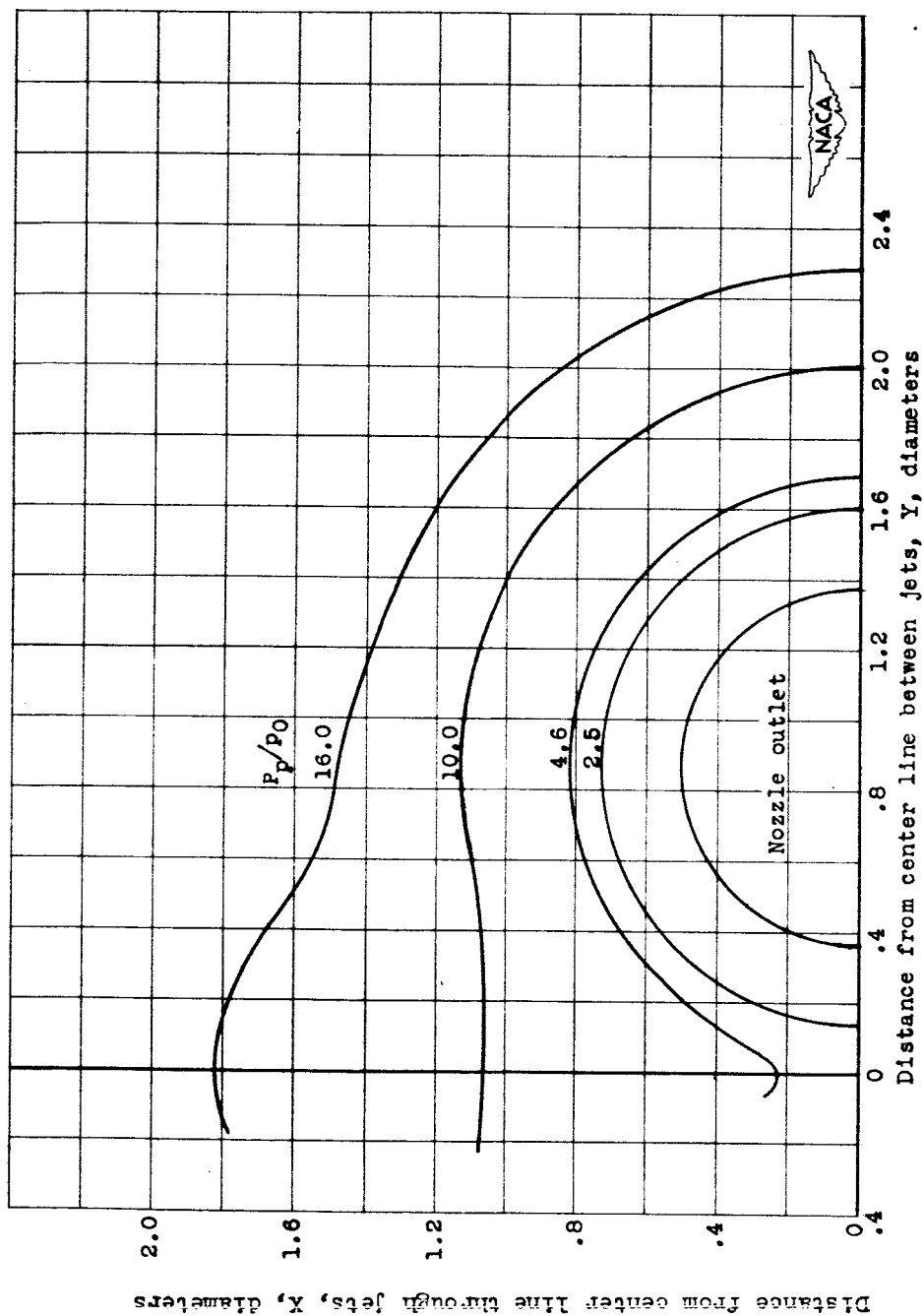


Figure 12. - Comparison of lateral boundaries of single and twin jets. Nozzle pressure ratio  $P_p/P_0$ , 16.0; Mach number ratio  $M/M_j$ , 0.11; axial station Z, 1 diameter.



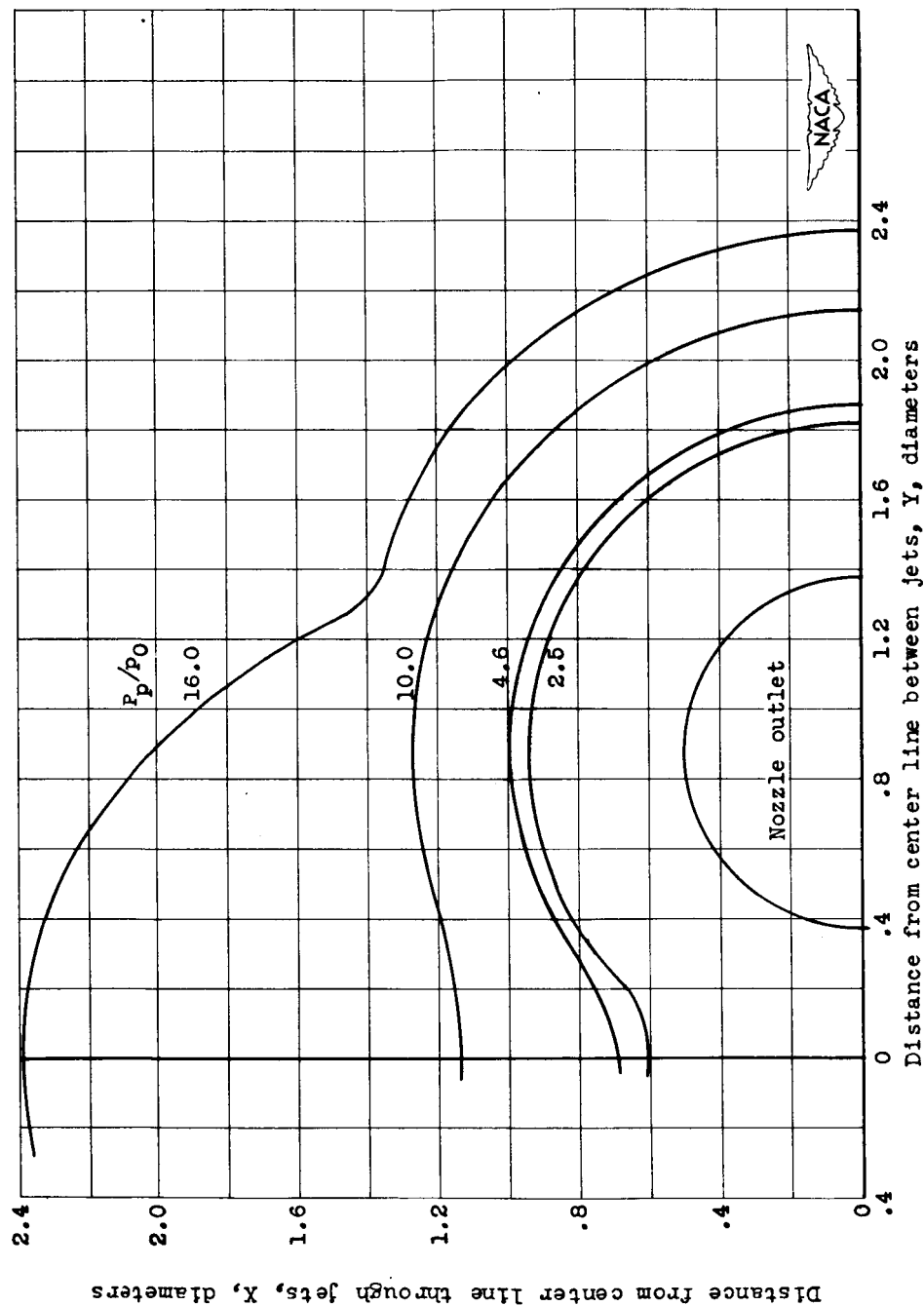
(a) Axial station  $Z$ , 1 diameter.

Figure 13. - Lateral boundaries for twin jets. Spacing between center lines  $S/D_n$ , 1.738 diameters; Mach number ratio  $M/M_j$ , 0.11.



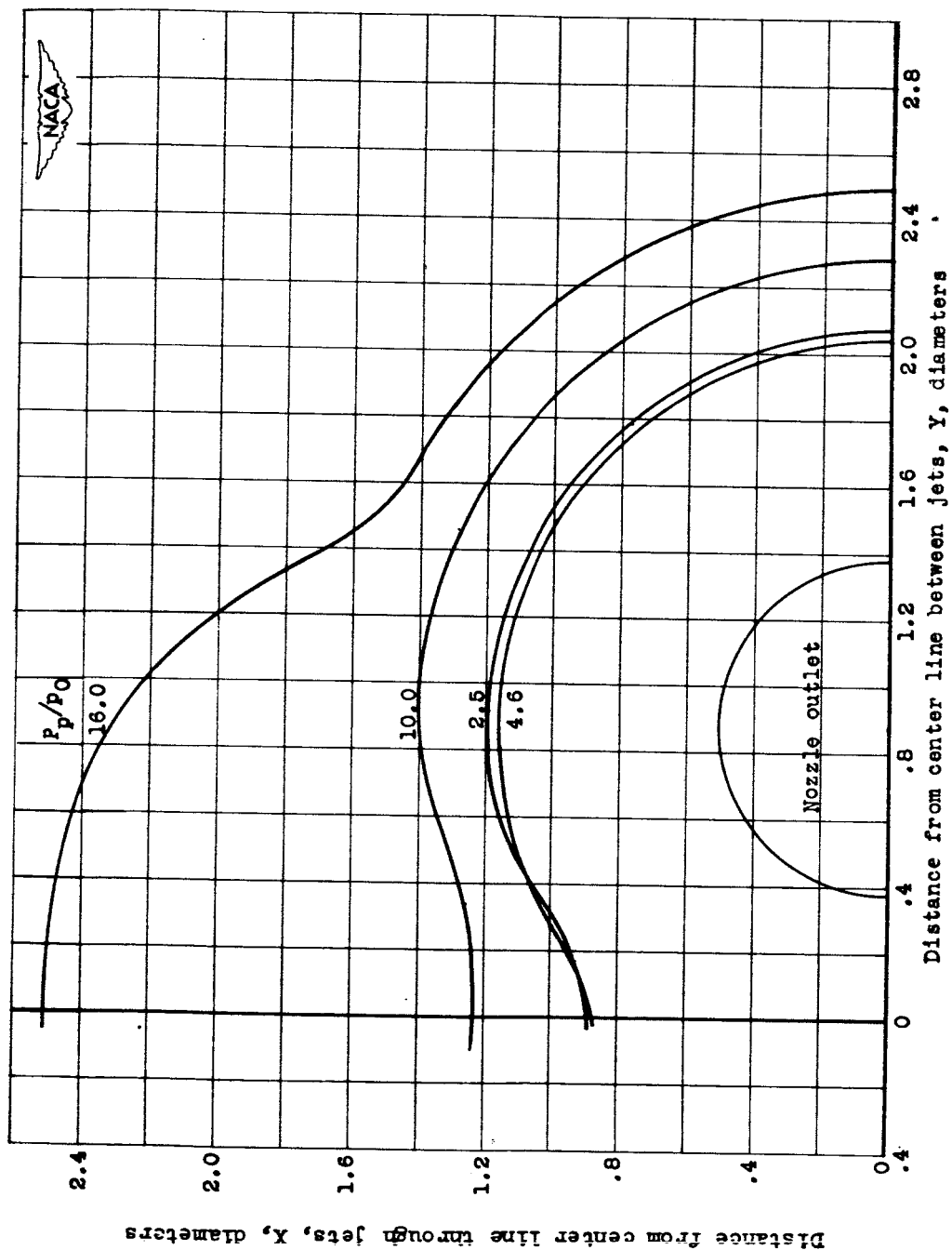
(b) Axial station Z, 2 diameters.

Figure 13. - Continued. Lateral boundaries for twin jets. Spacing between center lines  $S/D_n$ , 1.738 diameters; Mach number ratio  $M/M_j$ , 0.11.



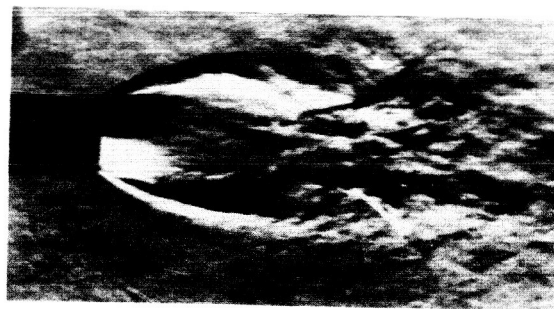
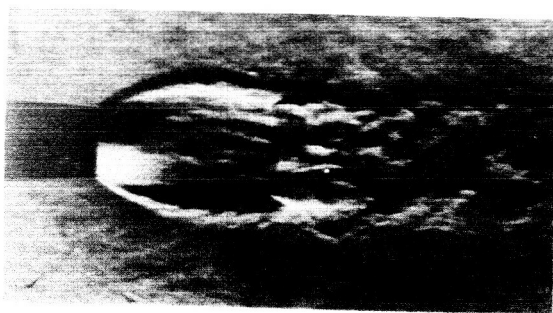
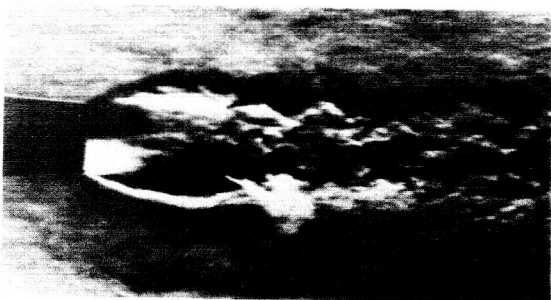
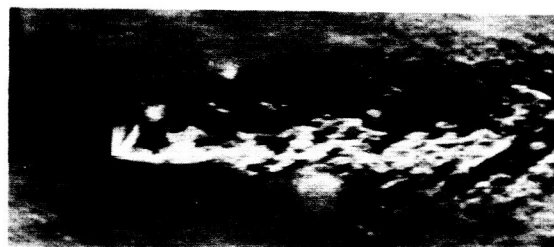
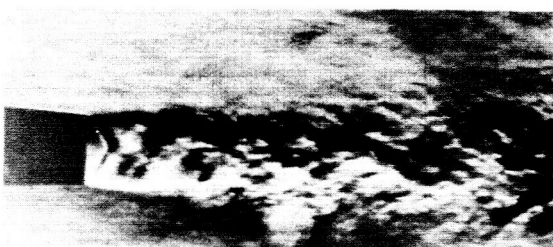
(c) Axial station  $Z$ , 4 diameters.

Figure 13. - Continued. Lateral boundaries for twin jets. Spacing between center lines  $S/D_n$ , 1.738 diameters; Mach number ratio  $M/M_j$ , 0.11.



(d) Axial station  $Z$ , 6 diameters.

Figure 13. - Concluded. Lateral boundaries for twin jets. Spacing between center lines  $S/D_n$ , 1.738 diameters; Mach number ratio  $M/M_j$ , 0.11.

Nozzle pressure ratio  $P_p/P_0$ , 16.0Nozzle pressure ratio  $P_p/P_0$ , 10.0Nozzle pressure ratio  $P_p/P_0$ , 4.6.Nozzle pressure ratio  $P_p/P_0$ , 2.5.

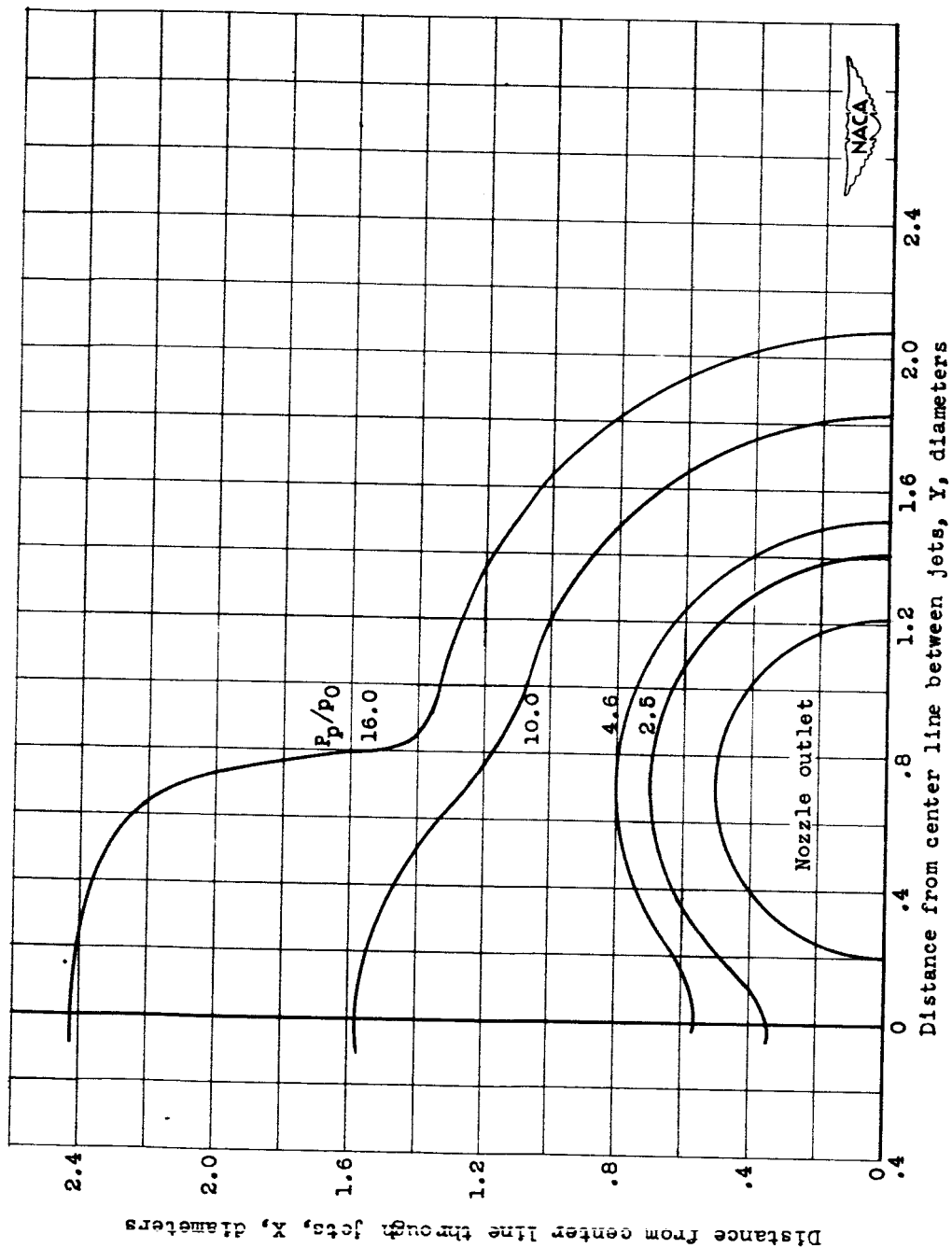
NACA  
C-255773  
5-2-50

(a) Single jet.

(b) Twin jets; spacing between center lines  $S/D_n$ , 1.42.

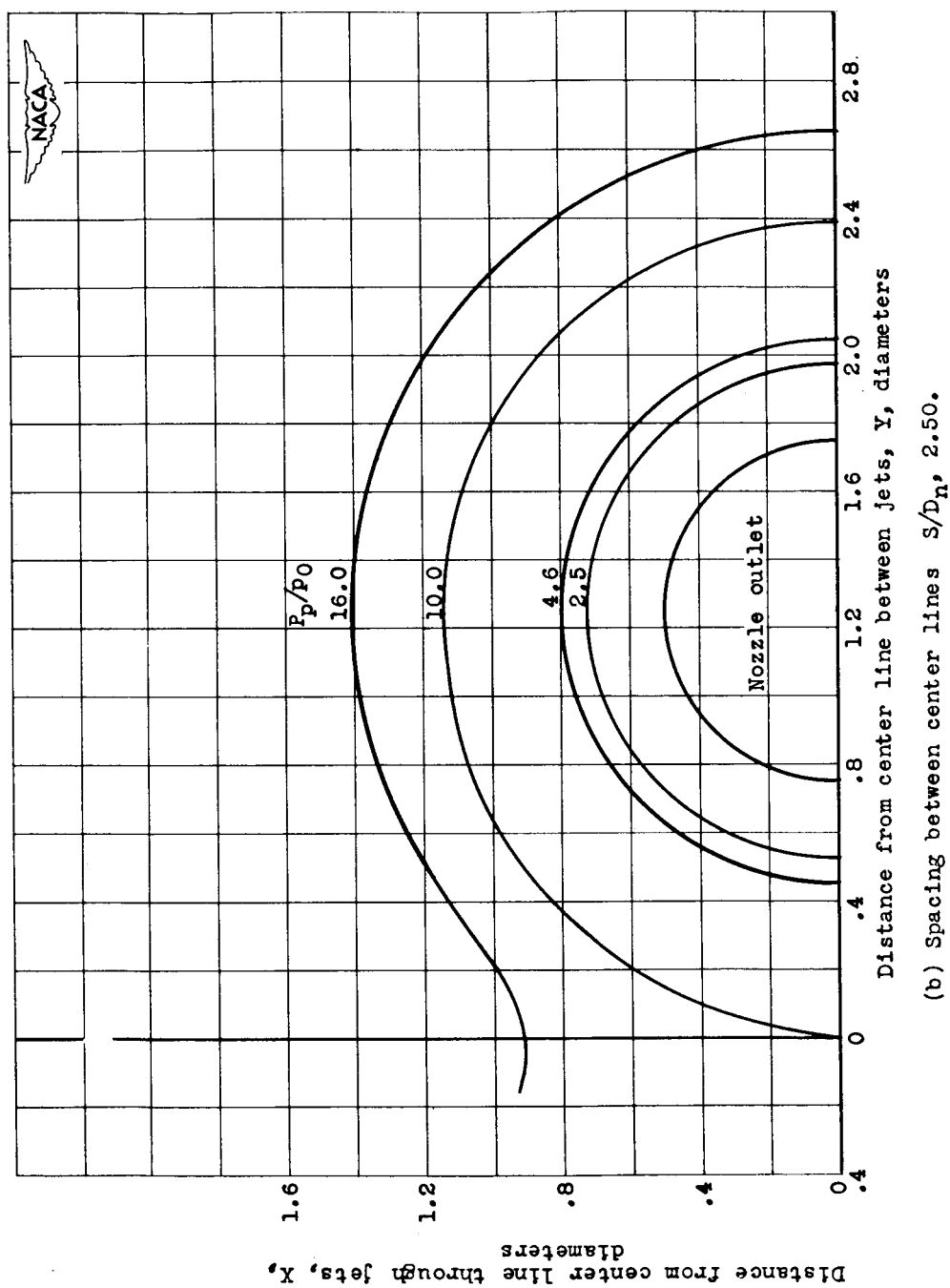
Figure 14. - Schlieren photographs of single and twin jets.





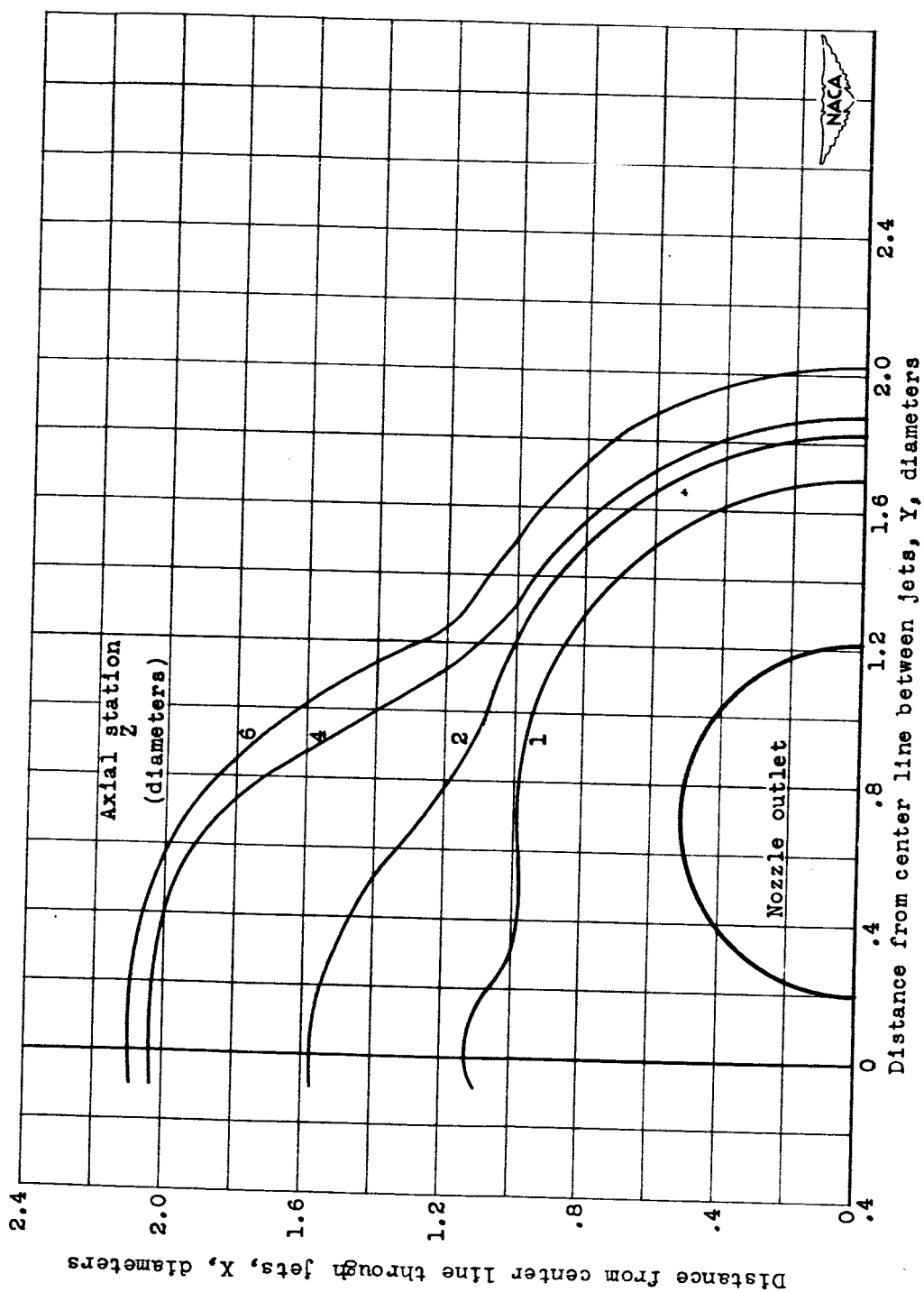
(a) Spacing between center lines  $S/D_n$ , 1.42.

Figure 15. - Lateral boundaries for twin jets. Mach number ratio  $M/M_j$ , 0.11; axial station  $Z$ , 2 diameters.



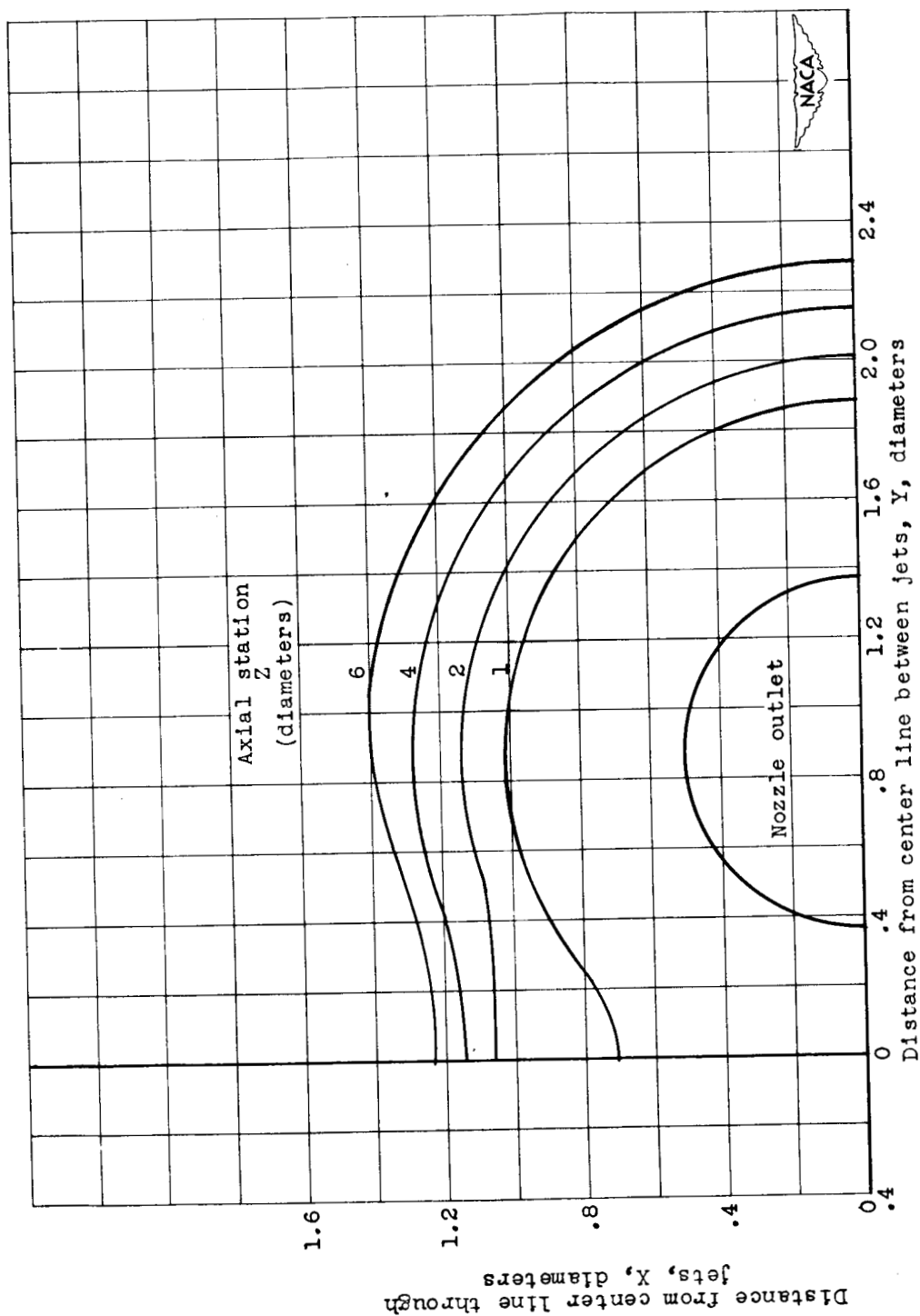
(b) Spacing between center lines  $S/D_n$ , 2.50.

Figure 15. - Concluded. Lateral boundaries for twin jets. Mach number ratio  $M/M_j$ , 0.11; axial station  $Z$ , 2 diameters.

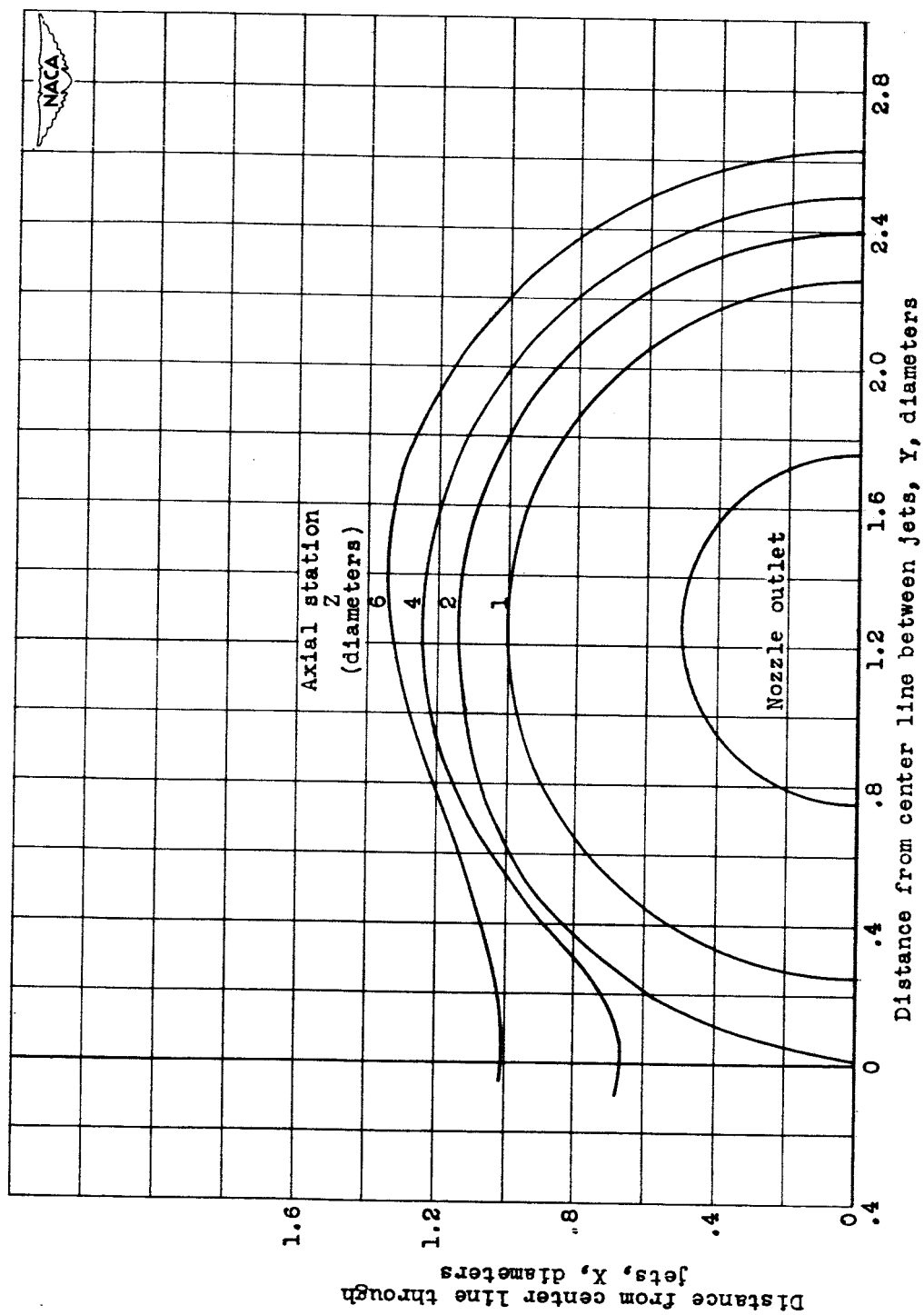


(a) Spacing between center lines  $S/D_n$ , 1.42.

Figure 16. - Lateral boundaries for twin jets. Nozzle pressure ratio  $P_p/P_0$ , 10.0; Mach number ratio  $M/M_j$ , 0.11.

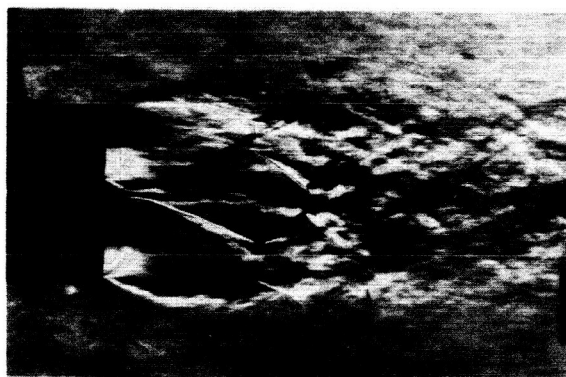
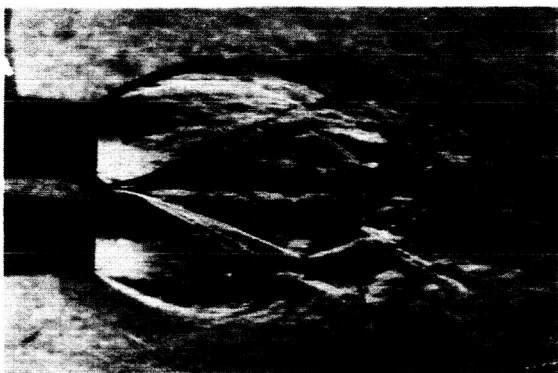


(b) Spacing between center lines  $S/D_n$ , 1.738.  
 Figure 16. - Continued. Lateral boundaries for twin jets. Nozzle pressure ratio  $P_p/P_0$ , 10.0; Mach number ratio  $M/M_j$ , 0.11.

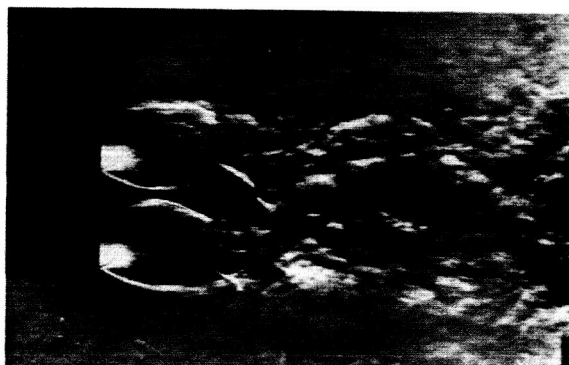
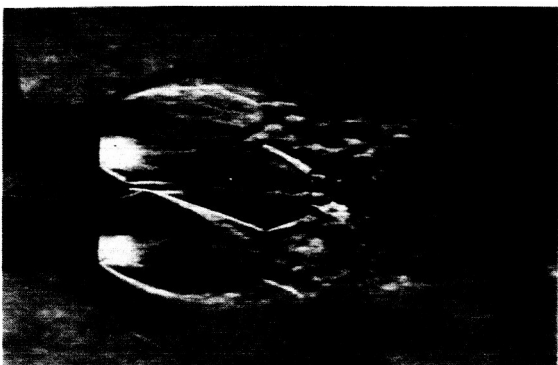


(c) Spacing between center lines  $S/D_n$ , 2.5.

Figure 16. - Concluded. Lateral boundaries for twin jets. Nozzle pressure ratio  $P_p/P_0$ , 10.0; Mach number ratio  $M/M_j$ , 0.11.



Spacing between center lines  $S/D_n$ , 1.42.



Spacing between center lines  $S/D_n$ , 1.738.



Spacing between center lines  $S/D_n$ , 2.5



C-25774  
5-2-50

(a) Nozzle pressure ratio,  
 $P_p/P_0$ , 16.0

(b) Nozzle pressure ratio,  
 $P_p/P_0$ , 10.0

Figure 17. - Schlieren photographs showing vertical view of twin jets for three nozzle spacings.

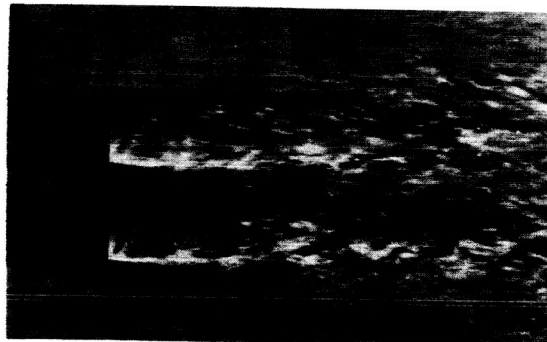
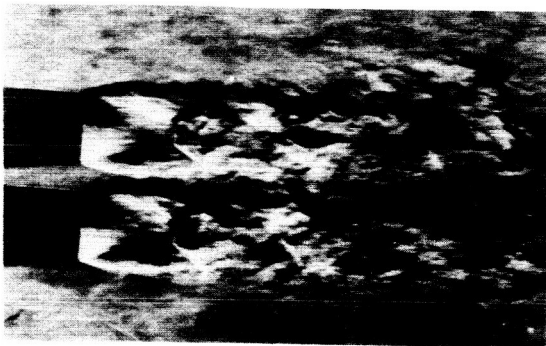
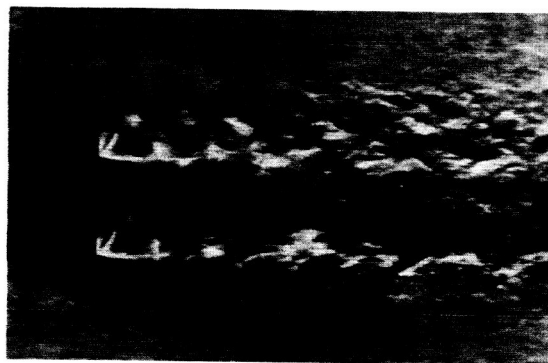
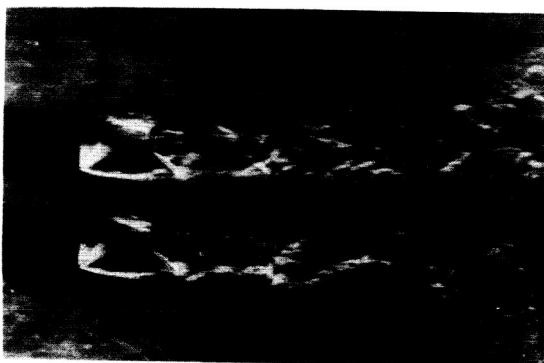
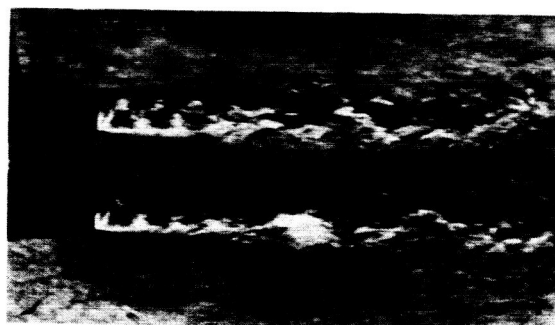
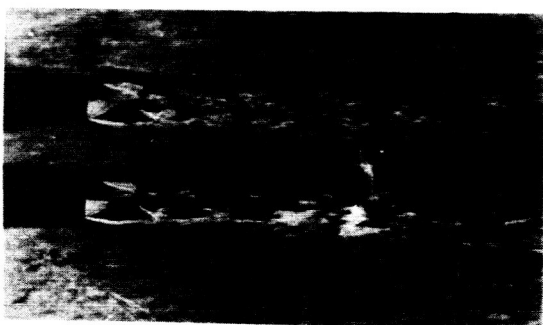
spacing between center lines  $S/D_n$ , 1.42Spacing between center lines  $S/D_n$ , 1.738.Spacing between center lines  $S/D_n$ , 2.5.C-25775  
5-2-50(c) Nozzle pressure ratio,  
 $P_p/P_0$ , 4.6.(d) Nozzle pressure ratio,  
 $P_p/P_0$ , 2.5.

Figure 17. - Concluded. Schlieren photographs showing vertical view of twin jets for three nozzle spacings.